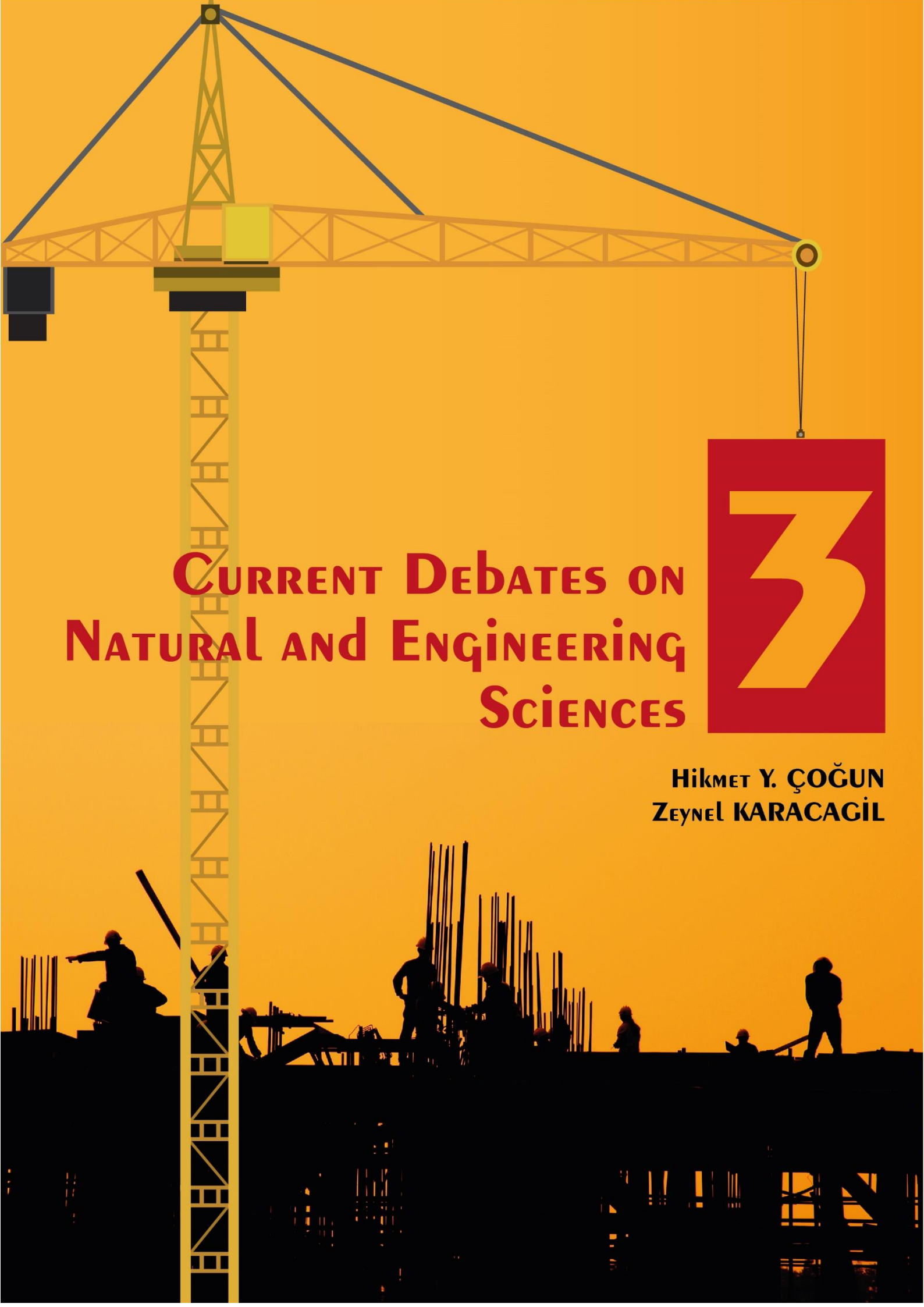

Current Debates on Natural and Engineering Sciences

3

Hikmet Y. ÇOĞUN
Zeynel KARACAGİL

ISBN: 978-625-7799-53-9

1st Edition

25 Haziran 2022

Current Debates on Natural and Engineering Sciences 3

Editors

Hikmet Y. ÇOĞUN

Zeynel KARACAGİL

Publisher
Engin DEVREZ
Bilgin Kültür Sanat Yayınları
Certificate No: 20193
Selanik Cd. No: 68/10 06640 Kızılay / Ankara
Phone: 0 (312) 419 85 67 – Fax: 0 (312) 419 85 68
www.bilginkultursanat.com
bilginkultursanat@gmail.com

Late Silurian-Middle Devonian Elemental and Carbon, Oxygen Isotope Geochemistry in the Bozdağ Limestones of Yükselen District (Konya, Türkiye) Around

Ali Müjdat ÖZKAN
Engin ÖZDEMİR

Introduction

The principal purpose of the investigation was to wield geochemical data obtained from samples to generate geochemistry for Late Silurian-Middle Devonian the Bozdağ Formation carbonates situated in the southeast of the Yükselen District (Konya, Turkey) in the Kütahya-Bolkardağı Belt (Fig. 1). Typically, the purpose of this geochemistry approximation is to describe elements and element ratios that alter through time and that permit sediments of the same age to be correlated or to differentiate sediments that are asynchronous. These alterations will then be used to form a stratigraphic framework.

The seawater geochemistry has been registered by the chemical composition of the sediments (by major and trace element distribution) and by the isotopic ratios of specific elements (Tsegab and Sum, 2019). Elemental and stable isotope geochemistry, including carbon and oxygen isotopes, is the most widely applied geochemical tool for the Neoproterozoic and Phanerozoic to investigate the rock record, such as reconstructing paleoenvironments, determining the tectonic setting of sedimentary basins, indirect dating and establishing regional or global correlations (Delpomdor and Préat, 2013). As Delpomdor and Préat (2013) stated, a very important issue in any study of carbonate geochemistry is whether a primary marine marker is protected. The Bozdağ limestones in our study area have undergone a rather minor alteration. Therefore, the Bozdağ limestones are quite suitable for geochemistry study.

A Survey of rare earth elements' attitudes and their normalized dispersion models during geochemical processes supply valuable knowledge about carbonate sediments and pale conditions of depositional settings (Abedini et al., 2018). The rare earth element dispersion models in seawaters and marine sediments are usually checked by many factors such as terrestrial material by the reason of weathering, hydrothermal activities, scavenging, oxygen fugacity, closeness to source lithologies, deposition due to biogenic conditions, and diagenesis (Abedini et al., 2018).

Geochemical studies and especially Phanerozoic climate changes have been a subject of worldwide interest recently. There is no detailed geochemical study of the Bozdağ Formation carbonates in the region. Therefore, a detailed geochemical study was needed for the Bozdağ Formation carbonates in the region. Because the Bozdağ carbonates are widespread in the region, they are very important materials to illuminate the geological development of the Late Silurian-Middle Devonian time interval.

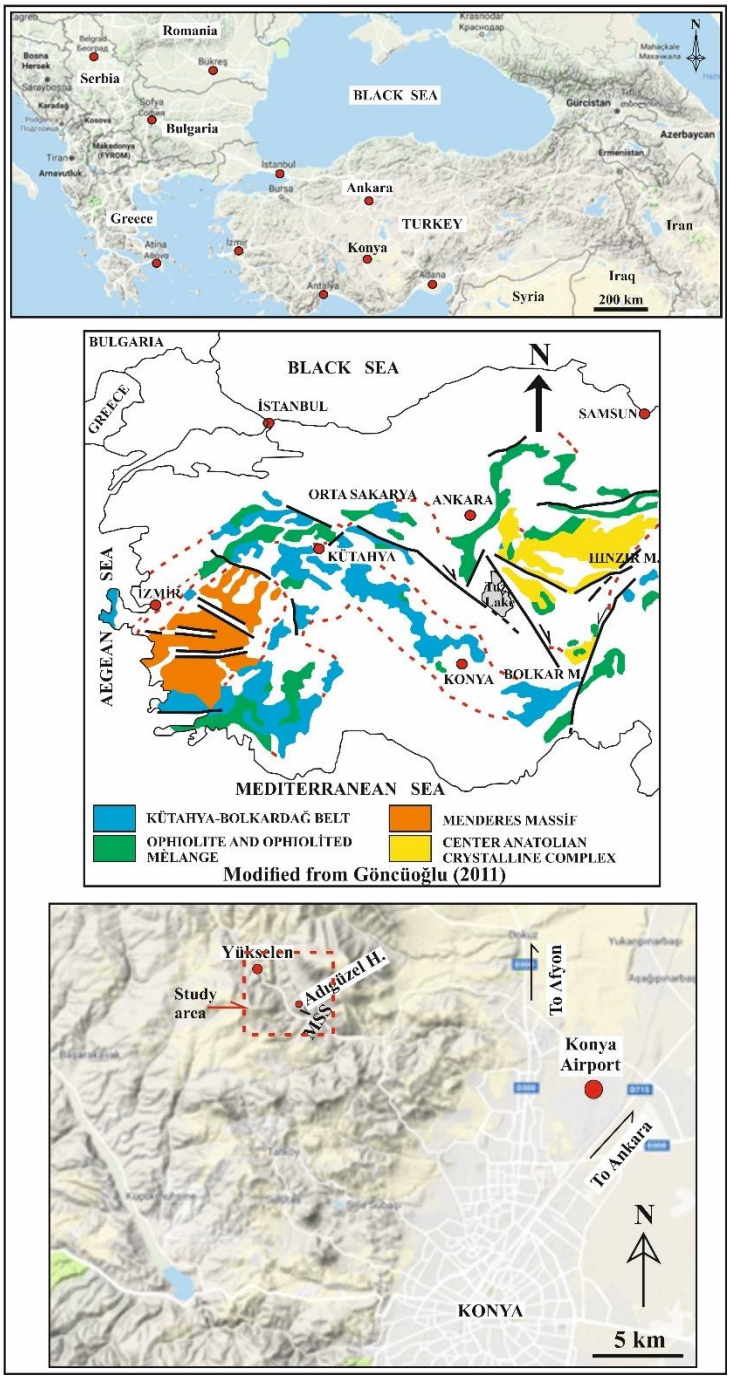

Figure. 1. Location map of the study area (Google Maps: https://www.google.com/maps/@38.0369777,32.4285516,11.25z/data=!5m1!1e4)

Geological Setting

The Bozdağ Formation, which outcrops in the eastern part of the study area and forms the basis, was named by Eren (1993) (Figs. 2,3).

The Bozdağ Formation, which includes dolostone at the base, consists mainly of limestones and is also observed as crystallized limestones and marbles in the region. The Bozdağ carbonates offer medium-thick stratification in black, gray, light gray, cream, and white. Offering some levels of lamination, the Bozdağ limestones also form coral and stromatoporoid (Fig. 4) patch reefs.

These carbonates, which mostly show biostromal properties, also contain carried stromatolite fragments (Eren, 1993). The Bozdağ Formation is medium to thick (Figs. 4b, 4c, 4d), at some levels very thick layered, gray at the lower levels, and light gray and white at the upper levels. The Bozdağ limestones contain some levels of laminated (Figs. 4b, 4d) and some levels of stromatoporoid bioherms (Fig. 4e).

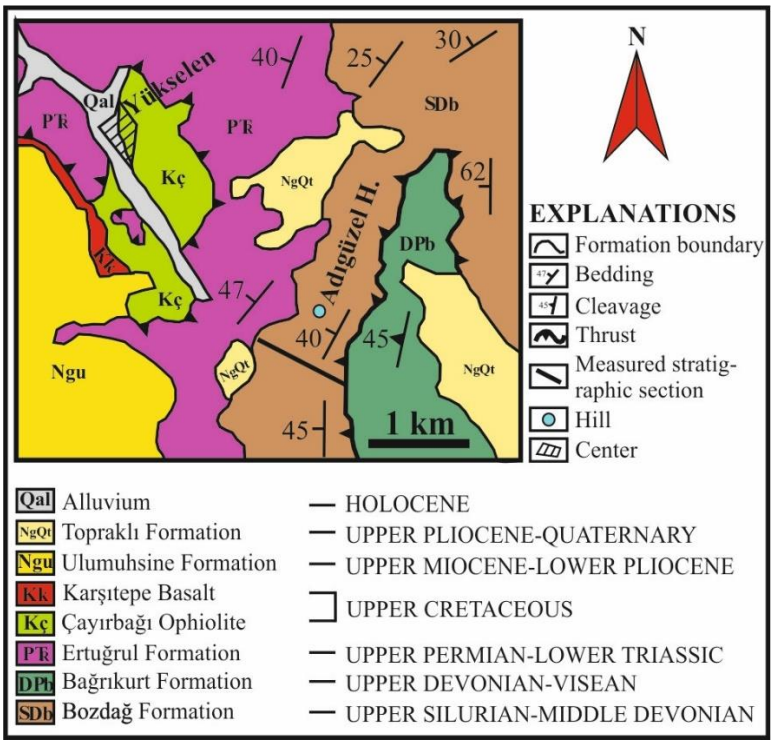

Figure 2. Geological map of the study area (modified from Eren, 1996).

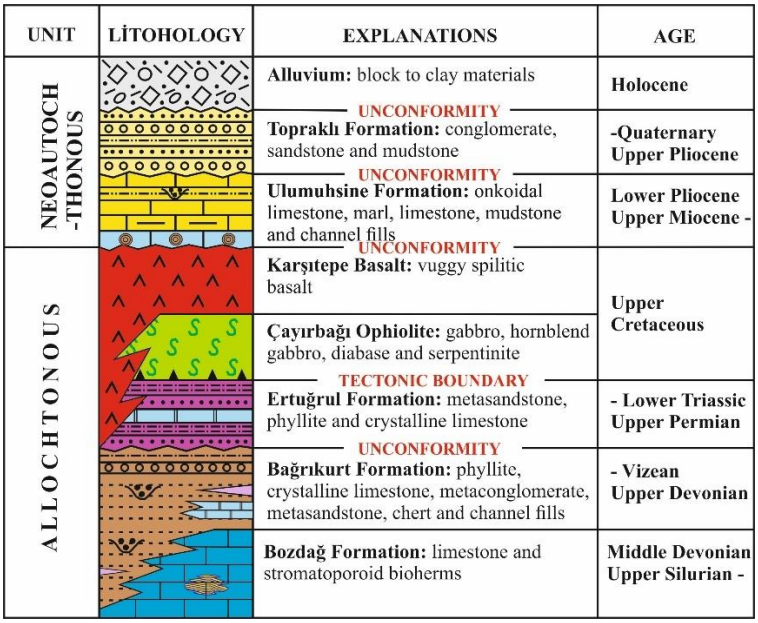

Figure 3. Stratigraphic column section of the study area (unscaled; modified from Eren, 1996)

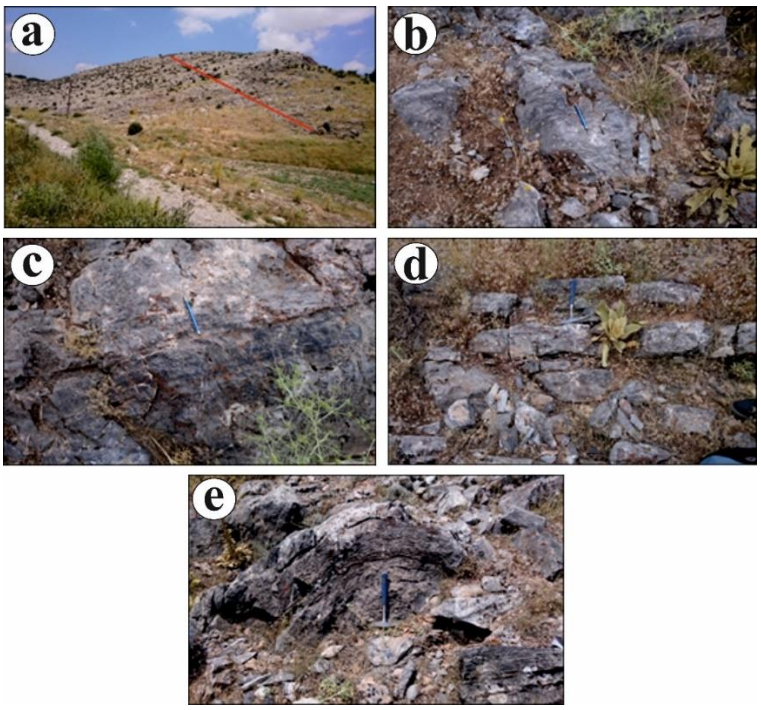

Figure 4. a) Bozdağ Formation measured stratigraphic section line (red line), b) Laminated and thick-bedded limestone (scale: pen, 14 cm), c) Medium-thick bedded limestone (scale: pen, 14 cm), d) Medium bedded limestone (scale: hammer, 28 cm), e) Stromatoporoid bioherm in the Bozdağ limestone (scale: hammer, 28 cm).

According to microscopic examinations, the Bozdağ limestone samples are mudstone, wackestone, packstone, dirty wackestone, laminated mudstone, and boundstone (according to Dunham, 1962).

The lower boundary of the Bozdağ Formation has tectonic contact with the Bağrıkurt Formation in the study area (Fig. 2). It is unconformably overlain by the Upper Permian- Lower Triassic the Ertuğrul Formation and the Upper Pliocene-Quaternary the Topraklı Formation at its upper boundary. The thickness of the formation has been measured in the study area at 260 m and reaches 800 m (Özkan, 2016).

The age of the Bozdağ Formation is controversial; Eren (1993) gave the unit a Late Silurian-Lower Carboniferous and Göncüoğlu a Late Silurian-Middle Devonian age. In this study, the unit was accepted as the Late Silurian-Middle Devonian. The Bozdağ Formation has developed as a reef complex on a carbonate shelf.

Materials and Methods

Geochemical studies are an application of geochemical data to sediments of all ages and to any facies accumulated in various environments (Ratcliffe et al., 2010). Whole-rock quantitative data were obtained from limestone samples for 47 elements: 11 major elements (Al, Si, Ti, Fe, Mn, Ca, Mg, K, P, Na, and Cr), 32 minor and trace elements (Ba, Cd, Ga, Co, Cs, Cu, Hg, Mo, Nb, Ni, Pb, Hf, Rb, Ta, Sc, Sr, Th, U, V, Zn, and Zr) and 15 rare earth elements (La, Ce, Pr, Nd, Sm, Eu, Gd, Tb, Dy, Y, Ho, Er, Tm, Yb, and Lu).

The material of this study is composed of the Bozdağ Formation limestones. The 1/25.000 scaled geological map used during the study was taken from Eren (1996). In this study, 37 samples

were collected from the limestones belonging to the Late Silurian-Middle Devonian aged the Bozdağ Formation which were exposed in the vicinity of the Yükselen District (Konya) along the measured section line. These 37 samples selected for geochemical examination were collected by taking into consideration the lithofacies characteristics and taking photographs from interesting localities.

The features of the outcrop enable a very detailed study of the main vertical facies successions and specify the environments of deposition. For the geochemical characterization of the Bozdağ limestone samples, mudstones and wackestones-packstones have been selected as they are thought to keep their original isotopic composition due to their lower permeability character in comparison to associated grain-supported rocks. Before oxygen and carbon isotopic analysis, the number of diagenetic phases in each sample was evaluated by a combination of petrographic observations and ICP analysis. Petrography analyses were applied on 37 thin sections stained with alizarin red to differentiate calcite from other carbonate minerals, and they were as well investigated under a petrographic microscope. 27 of the collected samples were sent to Acme Analytical Laboratory (Canada) for making analysis of main, trace, and rare earth elements, and they were read in ICP-ES/ICP-MS devices, and data was presented in ppm.

37 of the limestone samples of the Bozdağ Formation were sent to the University of California Santa Cruz laboratory for the determination of stable isotope analysis of $\delta^{13}C$ and $\delta^{18}O$, and ThermoScientific MAT-253 double input isotope ratio mass spectrometry (IRMS) combined with a separate vial of the acid drop using the ThemoScientific Kiel IV carbonate device was read with acid digestion. All data obtained as a result of field and laboratory studies are evaluated together with the literature and presented as a report.

The values that cannot be measured in the analysis of some elements were used as limit values in statistical evaluations.

Results

Geochemistry and Mineralogy

The mineralogical properties of the elements can be determined by geochemical data and existing mineralogical data. In addition, element-mineral connections can be created using graphical and statistical techniques. Fig. 6 shows the element distribution based on geochemical analysis data. In Fig. 6, Si, Al, K, P, Mn, REE, Rb, Sr, Zr, and Y elements are observed in relation to each other, while the Ca element exhibits unrelated to these elements. This indicates the difference between the carbonate and the detrital phase.

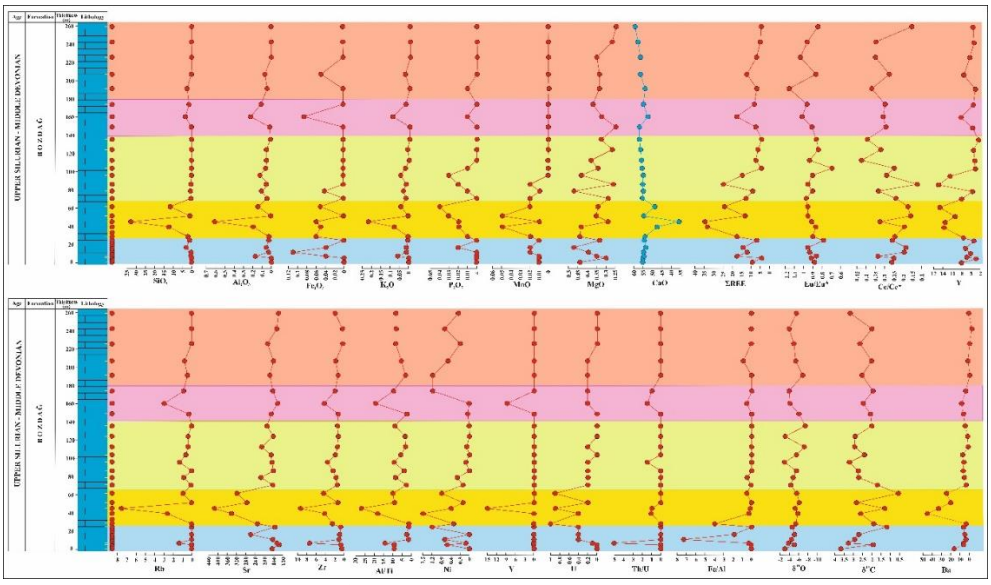

Figure 6. Petro-chemostratigraphic changes of the Bozdağ Formation limestone samples.

Statistical Techniques (Principal Component Analysis)

PCA analysis is a statistical technique used to recognize significant element associations, as elements originating together in the same area of the eigenvector plots have similar distributions and are likely to have similar mineralogical affinities. Fig. 7 shows the results of the Varimax rotated factor matrix of the Bozdağ limestone samples. Five components explained ~92% of the total variance in the 27 limestone samples analyzed.

(a)

Variable	Component Matrix PC 1	PC 2	PC 3	PC 4	PC 5
SiO_2	0.866	-0.435	0.111	-0.100	-0.071
Al_2O_3	0.811	-0.546	0.088	0.106	0.077
Fe_2O_3	0.280	0.028	0.358	0.794	-0.183
MgO	0.087	0.267	0.562	0.087	0.684
CaO	-0.878	0.417	-0.135	0.079	0.042
K_2O	0.817	-0.545	-0.049	0.089	0.084
Ba	0.813	-0.012	0.291	-0.325	0.033
Rb	0.784	-0.580	-0.062	0.101	0.085
Sr	0.799	-0.142	0.329	-0.268	0.110
Zr	0.783	-0.346	-0.154	0.207	0.093
Y	0.866	0.397	-0.209	-0.088	0.013
La	0.949	0.273	0.005	0.025	-0.013
Ce	0.918	-0.223	-0.005	0.168	0.163
Pr	0.977	0.138	0.022	0.034	0.004
Nd	0.975	0.153	0.044	0.034	0.006
Sm	0.974	0.111	-0.004	0.036	-0.016
Eu	0.970	0.164	-0.043	0.042	-0.020
Gd	0.969	0.199	-0.051	0.023	-0.006
Tb	0.975	0.155	-0.090	0.022	0.015
Dy	0.952	0.265	-0.107	-0.011	-0.009
Ho	0.965	0.205	-0.121	-0.014	0.004
Er	0.945	0.244	-0.156	-0.077	0.039
Tm	0.952	0.188	-0.177	-0.065	0.015
Yb	0.958	0.158	-0.166	-0.103	0.023
Lu	0.941	0.123	-0.212	-0.032	0.049
LOI	-0.849	0.449	-0.099	0.140	0.092
Co	0.613	0.317	0.601	0.074	0.017
Pb	0.573	-0.150	0.038	0.144	-0.450
Ni	0.198	-0.088	0.599	-0.304	-0.449
Zn	0.482	0.661	0.034	0.113	-0.268
Eigen values:	20.772	2.951	1.650	1.120	1.068
%Variance explained :	69.239	9.837	5.500	3.733	3.560
%Cumulative variance :	69.239	79.076	84.576	88.310	91.870

(b)

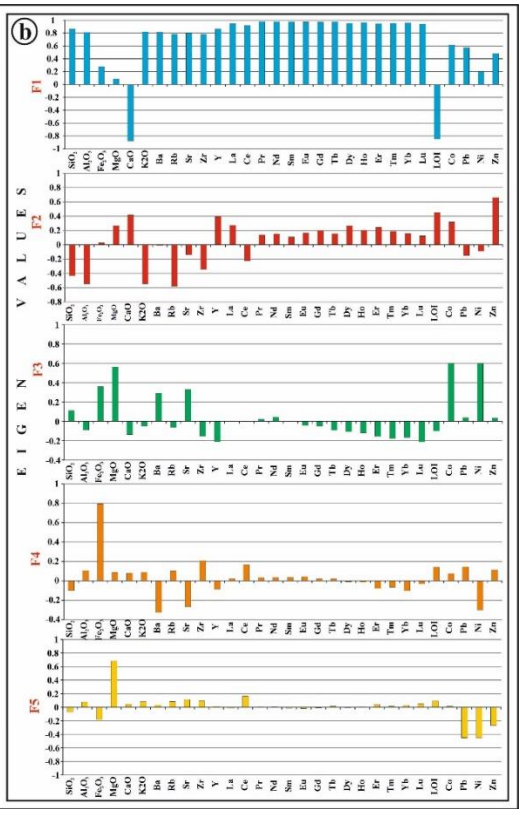

Figure 7. Principal component loadings (A), Graphical representation of the scaled, and ordered eigenvalues of PC for 30 elements analyzed (B).

The principal component scores for the original vectors (eigenvectors) demonstrate the association of particular elements and the relationship between some elements and mineralogy (Craigie, 2015). You can see the discussion of these relationships below.

Factor 1: includes Ca. This element is mainly concentrated in carbonate minerals. Factor 1: the first factor, corresponding to 69% of the change, is represented by the negative factor of CaO and LOI, while the other components are all represented by the positive factor. This situation is compatible with the differentiation of the CaO-LOI group from the other group in the cluster analysis diagram (Carbonate phase).

Factor 2: The second factor corresponding to about 10% of the change is represented by the positive factor of other components Zn, Co, LOI, CaO, MgO, Y, La, despite the significant negative loads of Si, Al, K, Rb, Zr, Ce (Aliminosilicate: detrital phase).

Factor 3: The third factor corresponding to 5.5% of the change is Al, CaO, K, Rb, Zr, Y, Eu, Gd, Tb, Dy, Ho, Er, Tm, Yb, Lu, against negative loadings of LOI, other it is represented by the important positive factor of the components Si, Fe, MgO, Ba, Sr, Ni, Co (Clay: REE phase).

Factor 4: The fourth factor corresponding to 4% of the change is the negative load's Si, Ba, Sr, Y, Er, Tm, Yb, Lu, Ni, while the other components are Al, Fe, Mg, Ca, K, Rb, Zr, Ce LOI, Co, Pb, Zn are represented by a positive factor (Silicate: detrital phase).

Factor 5: The fifth factor corresponding to 3.5% of the change is represented by the positive factor of the other components MgO, Ce, compared to the negative loads of Si, Fe, Pb, Ni, and Zn.

The result of the hierarchical cluster analysis was presented as a dendrogram (Fig. 8). The carbonate and detrital phases are evident in the dendrogram. The detrital phase is also divided into two subgroups.

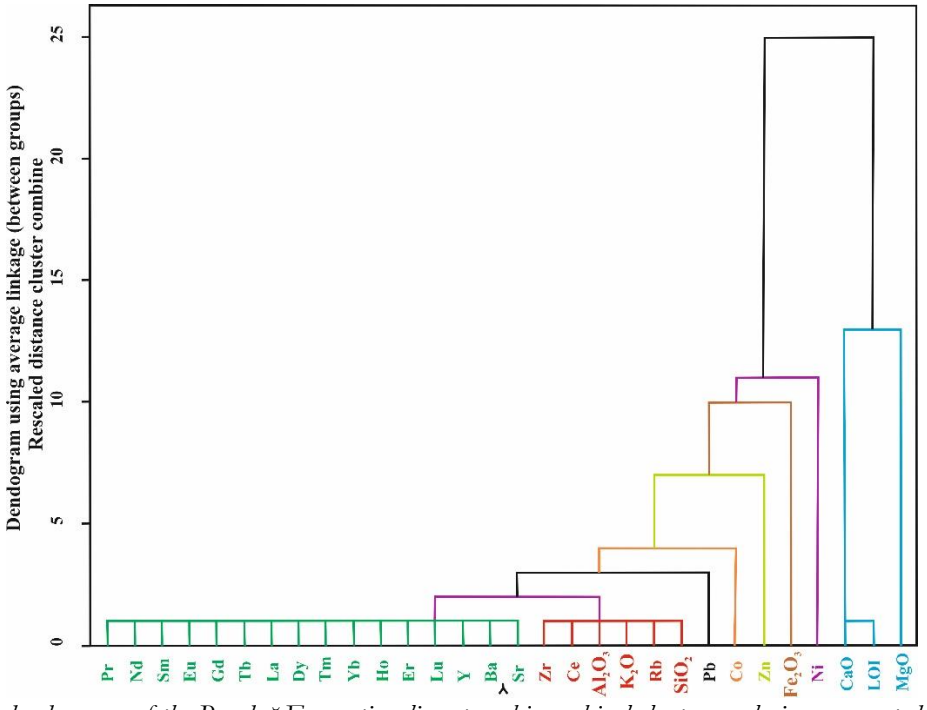

Figure 8. The dendrogram of the Bozdağ Formation limestone hierarchical cluster analysis was created using the Ward method.

Graphical Techniques (Binary Diagrams)

Although PCA is used in many studies to establish the element: mineral connection, abnormally high and low values of some elements (Craig, 2015) may cause some errors. Therefore, it is important to support the interpretation of statistical data using binary diagrams. The binary diagram results are shown in Table 1.

Table 1. Major (%) and trace element (ppm) correlation of the Bozdağ Formation limestones

	SiO2	Al2O3	Fe2O3	MgO	CaO	K2O	Na2O	P2O5	MnO	TiO2	Cr2O3	Ba	Rb	Sr	Zr	Y	Co	Pb	Ni	Zn	Ga	Cs	Ta	Th	Nb	Hf	Mo	U	V	Sc	Cu	TREE
SiO2	1																															
Al2O3	0.82	1																														
Fe2O3	0.05	0.06	1																													
MgO	0	0	0.02	1																												
CaO	0.99	0.82	0.06	0	1																											
K2O	0.84	0.99	0.06	0	0.85	1																										
Na2O	0	0	0	0	0	0	1																									
P2O5	0.11	0.05	0	0.03	0.12	0.06	0	1																								
MnO	0.03	0	0.01	0.05	0.04	0	0	0.18	1																							
TiO2	0.77	0.76	0.03	0.03	0.76	0.77	0	0.01	0.01	1																						
Cr2O3	0	0	0	0	0	0	0	0	0	0	1																					
Ba	0.57	0.37	0.01	0.03	0.59	0.42	0	0.22	0.39	0.21	0	1																				
Rb	0.80	0.98	0.07	0	0.81	0.98	0	0.04	0	0.75	0	0.37	1																			
Sr	0.72	0.43	0.01	0.06	0.74	0.45	0	0.25	0.26	0.40	0	0.67	0.41	1																		
Zr	0.57	0.76	0.04	0	0.59	0.77	0	0.11	0	0.45	0	0.30	0.70	0.30	1																	
Y	0.32	0.25	0.02	0.01	0.34	0.25	0	0.54	0.25	0.12	0	0.46	0.21	0.35	0.31	1																
Co	0.21	0.06	0.17	0.16	0.24	0.09	0	0.12	0.56	0.04	0	0.45	0.05	0.43	0.11	0.25	1															
Pb	0.35	0.26	0.05	0.01	0.34	0.26	0	0.07	0	0.29	0	0.16	0.22	0.24	0.23	0.16	0.12	1														
Ni	0.08	0.02	0.02	0	0.08	0.02	0	0	0.04	0	0	0.13	0.02	0.06	0	0	0.09	0.01	1													
Zn	0.03	0	0.05	0.02	0.04	0	0	0.51	0.22	0.01	0	0.11	0	0.09	0.05	0.47	0.25	0.16	0	1												
Ga	0	0	0	0	0	0	0	0	0	0	0	0	0	0	0	0	0	0	0	0	1											
Cs	0.75	0.83	0.07	0.03	0.74	0.82	0	0.01	0.01	0.94	0	0.19	0.84	0.34	0.49	0.12	0.02	0.25	0	0.01	0	1										
Ta	0	0	0	0	0	0	0	0	0	0	0	0	0	0	0	0	0	0	0	0	0	0	1									
Th	0.68	0.86	0.03	0	0.70	0.90	0	0.03	0	0.71	0	0.34	0.83	0.33	0.81	0.19	0.10	0.25	0	0	0	0.71	0	1								
Nb	0.39	0.52	0.02	0	0.40	0.54	0	0	0.04	0.56	0	0.18	0.52	0.13	0.38	0.07	0.01	0.11	0.04	0.05	0	0.60	0	0.54	1							
Hf	0.34	0.52	0	0.01	0.36	0.55	0	0	0.02	0.48	0	0.10	0.45	0.12	0.70	0.05	0.04	0.20	0.01	0	0	0.44	0	0.78	0.46	1						
Mo	0.02	0	0	0.20	0.02	0	0	0.03	0.14	0	0	0.06	0	0.12	0	0.02	0.17	0.03	0	0.04	0	0	0	0	0.01	0.01	1					
U	0.45	0.22	0.14	0.06	0.46	0.22	0	0.15	0.05	0.23	0	0.23	0.20	0.50	0.24	0.25	0.44	0.25	0.09	0.21	0	0.21	0	0.14	0.05	0.06	0.02	1				
V	0.77	0.81	0.05	0.03	0.76	0.81	0	0.01	0.01	0.98	0	0.20	0.81	0.37	0.48	0.12	0.03	0.27	0	0.01	0	0.99	0	0.72	0.59	0.46	0	0.22	1			
Sc	0.77	0.76	0.03	0.03	0.76	0.77	0	0.01	0.01	1	0	0.21	0.75	0.40	0.45	0.12	0.04	0.29	0	0.01	0	0.94	0	0.71	0.56	0.48	0	0.23	0.98	1		
Cu	0.56	0.39	0.07	0.03	0.58	0.39	0	0.12	0.09	0.49	0	0.29	0.36	0.59	0.23	0.20	0.33	0.51	0.01	0.13	0	0.44	0	0.36	0.16	0.20	0.24	0.38	0.47	0.49	1	
TREE	0.59	0.52	0.08	0.02	0.61	0.53	0	0.26	0.24	0.27	0	0.60	0.48	0.53	0.55	0.79	0.42	0.27	0.03	0.29	0	0.29	0	0.46	0.15	0.20	0.07	0.40	0.29	0.27	0.40	1

Red numbers are negative values.

In Table 1, the strong positive relationship is shown in the Al versus K crossplot (R: 0.99), Al versus Rb crossplot (R: 0.98), Al versus Cs crossplot (R: 0.88), Al versus Th crossplot (R: 0.86), Al versus Si crossplot (R: 0.82), Al versus V crossplot (R: 0.81), Al versus Ti crossplot (R: 0.76), Al versus Zr crossplot (R: 0.76), Al versus Sc crossplot (R: 0.76) deduces that these elements are concentrated in clay minerals. The strong negative correlation of these elements with Ca indicates that they are not related to the carbonate phase, but to the detrital phase (by carbonate dilution). In addition, the fact that Ca does not positively correlate with any other element indicates that this element is related to calcite (carbonate phase). Interestingly, Mg does not correlate strong positive with any other element. So, Mg is probably related to dolomite. Again, the Fe element does not contain a strong positive correlation with any other element. This leads us to the interpretation that the element Fe is taken from Fe-oxyhydroxides. Na does not correlate with any other element. Thus, the element Na suggests obtaining from plagioclase feldspar and/or smectite. Since P has moderate positive correlations with Y (R: 0.54), and Zn (R: 0.51), it probably suggests originating from clay minerals. Mn suggests that it originates from clay minerals, as it shows moderate to a weak positive correlation with Co (R: 0.56), and Ba (R: 0.39). Cr does not correlate with any other element. Therefore, the Cr element suggests being caused by heavy minerals such as chrome spinel. Since the Ba element exhibits moderate and weak positive correlations with Sr (R: 0.67), Y (R: 0.46), and Co (R: 0.45), it refers to originating from clay minerals. Zr element, shows high to medium positive correlation with Th (R: 0.81), K (R: 0.77), Al (R: 0.76), Hf (R: 0.70), Rb (R: 0.70), Si (R: 0.57), TREE (R: 0.55), Cs (R: 0.49), V (R: 0.48), Sc (R: 0.45). This means that the Zr element originates from some clay minerals as well as Zircon minerals. Total rare earth elements show high and medium positive correlation with Y (R: 0.79), Ba (R: 0.60), Si (R: 0.59), Zr (R: 0.55), K (R: 0.53), Sr (R: 0.53), Al (R: 0.52), and Rb (R: 0.48) elements. From here, we can say those rare earth elements are supplied from clays.

Key Elements and Ratios Used For Geochemical Aims

In this study, although data were presented for 45 elements (Table 2 to 5), most geochemical correlation schemes are generally based on variations in 4-12 'key' or 'index' elements (Craig, 2015). In this research, the framework is mainly based on variations in the 'stable' elements (e.g. Si, Th, Nb, Ti, Zr, Hf, Ta, Cr, Y, and REE) associated with heavy minerals and silicate as these are primarily uninfluenced by post-depositional weathering and/or diagenesis. Although the association of these elements (except Si) with heavy minerals has been stated in this investigation using statistical and graphical techniques, it is generally very difficult to determine precise mineralogical affinities. The exceptions to this are Zr and Hf which are nearly merely concentrated in detrital zircon (Craig, 2015).

Si is provided mainly by quartz, but it may be part of any silicate mineral too. For instance, the elements Ti, Ta, and Nb may be correlated with a variety of heavy minerals, including rutile, anatase, titanate, and opaque heavy minerals (as ilmenite, magnetite, titanomagnetite, rutile, anatase, sphene). Cr is most often supplied from chrome spinel, but it can also be found in opaque heavy minerals. The element Th is usually plenty in monazite but, considered the low abundance of this mineral in most sedimentary rocks, it is quite likely to be intensified in zircons, apatites, and weathered kaolinite (in association with Al, Ga, and Sc), and opaque heavy minerals. Y is most often supplied from apatite and monazite, but it can also be found in heavy minerals. REE is supplied from clay and mica, kaolinite or gibbsite (associated with high Al), Fe-oxyhydroxides, siderite, zircon, and garnet.

Table 2. Major element (%) concentrations of the Bozdağ Formation limestones

Sample	SiO_2	Al_2O_3	Fe_2O_3	MgO	CaO	Na_2O	K_2O	TiO_2	P_2O_5	MnO	Cr_2O_3	LOI	TOT/C	TOT/S
J-1	0.07	<0.01	<0.04	0.44	55.36	<0.01	<0.01	<0.01	<0.01	0.01	<0.002	44.1	12.53	<0.02
J-4	0.07	<0.01	<0.04	0.30	55.33	<0.01	<0.01	<0.01	<0.01	0.01	<0.002	44.2	12.53	<0.02
J-5	0.58	0.16	0.04	0.35	54.82	<0.01	0.06	<0.01	<0.01	0.01	<0.002	43.9	12.43	<0.02
J-8	0.27	0.02	0.11	0.39	55.06	<0.01	0.01	<0.01	<0.01	0.02	<0.002	44.1	12.72	<0.02
J-12	2.9	0.03	0.04	0.47	53.62	<0.01	0.01	<0.01	0.02	0.02	<0.002	42.8	12.20	<0.02
J-17	1.28	0.02	<0.04	0.34	54.78	<0.01	<0.01	<0.01	<0.01	0.01	<0.002	43.5	12.40	<0.02
J-19	2.37	0.02	0.06	0.44	53.94	<0.01	<0.01	<0.01	0.01	0.02	<0.002	43.1	12.37	<0.02
J-24	13.3	0.21	0.05	0.43	47.70	<0.01	0.08	0.01	0.02	0.05	<0.002	38.1	10.92	<0.02
J-28	33.0	0.62	0.06	0.29	36.64	<0.01	0.21	0.02	0.02	0.01	<0.002	29.0	8.38	<0.02
J-32	1.01	<0.01	<0.04	0.35	54.63	<0.01	<0.01	<0.01	0.03	0.05	<0.002	43.9	12.49	<0.02
J-37	11.6	0.12	0.05	0.34	48.97	<0.01	0.04	<0.01	0.04	0.02	<0.002	38.7	11.12	<0.02
J-42	0.36	0.03	<0.04	0.29	55.46	<0.01	0.01	<0.01	<0.01	0.02	<0.002	43.8	12.42	<0.02
J-47	0.53	0.10	0.04	0.47	55.11	<0.01	0.03	<0.01	0.01	0.01	<0.002	43.7	12.64	<0.02
J-52	0.42	0.05	<0.04	0.26	55.49	<0.01	0.01	<0.01	0.02	0.02	<0.002	43.7	12.55	<0.02
J-58	0.30	0.11	<0.04	0.43	55.11	<0.01	0.04	<0.01	0.04	<0.01	<0.002	43.9	12.36	<0.02
J-62	0.23	0.07	<0.04	0.34	55.34	<0.01	0.02	<0.01	0.01	<0.01	<0.002	43.9	12.58	<0.02
J-68	0.13	0.04	<0.04	0.38	55.57	<0.01	<0.01	<0.01	<0.01	<0.01	<0.002	43.8	12.45	<0.02
J-75	0.14	0.04	<0.04	0.27	55.71	<0.01	0.01	<0.01	<0.01	<0.01	<0.002	43.8	12.61	<0.02
J-82	0.04	<0.01	<0.04	0.32	55.86	<0.01	<0.01	<0.01	<0.01	<0.01	<0.002	43.8	12.54	<0.02
J-89	0.19	0.03	<0.04	0.25	55.77	<0.01	<0.01	<0.01	<0.01	<0.01	<0.002	43.7	12.65	<0.02
J-96	3.60	0.22	0.08	0.33	53.35	<0.01	0.07	0.01	0.01	<0.01	<0.002	43.3	12.08	<0.02
J-104	0.92	0.11	<0.04	0.37	55.04	<0.01	0.03	<0.01	<0.01	<0.01	<0.002	43.4	12.51	<0.02
J-114	2.00	0.04	<0.04	0.33	54.61	<0.01	0.01	<0.01	0.01	<0.01	<0.002	42.9	12.36	<0.02
J-124	0.17	0.07	0.05	0.33	55.64	<0.01	0.02	<0.01	<0.01	<0.01	<0.002	43.7	12.51	<0.02
J-134	0.11	<0.01	<0.04	0.36	55.66	<0.01	<0.01	<0.01	<0.01	<0.01	<0.002	43.8	12.63	<0.02
J-144	0.23	<0.01	<0.04	0.28	55.76	<0.01	<0.01	<0.01	<0.01	<0.01	<0.002	43.7	12.56	<0.02
J-154	0.04	<0.01	<0.04	0.25	56.01	<0.01	<0.01	<0.01	<0.01	<0.01	<0.002	43.7	12.68	<0.02

Table 3. Trace element (ppm) concentrations of the Bozdağ Formation limestones

Sample	Ba	Rb	Sr	Zr	U	V	Mo	Ni	Co	Th	Pb	Zn	Sc	Hf	Cu	Cs	Ga	Nb	Ta	Cd	Hg
J-1	17	<0.1	167	0.6	<0.1	<8	<0.1	<0.1	0.3	<0.2	0.6	1	<1	<0.1	0.8	<0.1	<0.5	0.3	<0.1	0.5	0.02
J-4	7	<0.1	138	0.7	<0.1	<8	<0.1	0.7	0.3	<0.2	0.6	2	<1	<0.1	1.1	<0.1	<0.5	<0.1	<0.1	0.5	0.18
J-5	7	1.4	145	7.5	0.1	<8	<0.1	0.1	0.4	0.5	1.2	3	<1	0.2	2.2	<0.1	<0.5	0.2	<0.1	0.5	0.06
J-8	4	<0.1	163	1.1	0.4	<8	<0.1	0.8	0.6	<0.2	1.4	5	<1	<0.1	6.5	<0.1	<0.5	<0.1	<0.1	0.3	0.31
J-12	5	<0.1	258	1.0	0.4	<8	0.3	<0.1	0.5	<0.2	1.5	4	<1	<0.1	12.6	<0.1	<0.5	<0.1	<0.1	0.4	0.17
J-17	7	<0.1	155	0.8	0.4	<8	<0.1	1.2	0.3	<0.2	0.9	3	<1	<0.1	5.4	<0.1	<0.5	<0.1	<0.1	0.3	0.15
J-19	4	<0.1	231	2.6	1.0	<8	<0.1	0.5	0.7	<0.2	1.0	3	<1	<0.1	4.0	<0.1	<0.5	<0.1	<0.1	0.2	0.29
J-24	45	2.7	344	4.1	0.4	<8	0.2	1.5	0.8	0.4	1.1	4	1	<0.1	6.6	0.1	<0.5	0.1	<0.1	0.2	0.10
J-28	33	7.6	416	9.4	0.9	15	<0.1	0.6	0.5	0.8	2.9	2	2	0.2	17.2	0.5	<0.5	0.4	<0.1	0.3	0.65
J-32	20	<0.1	275	1.4	0.2	<8	<0.1	0.2	0.6	<0.2	0.5	4	<1	<0.1	6.0	<0.1	<0.5	<0.1	<0.1	0.3	0.11
J-37	25	1.0	318	4.6	0.9	<8	<0.1	0.9	0.5	<0.2	1.8	8	<1	<0.1	5.0	<0.1	<0.5	<0.1	<0.1	0.5	0.27
J-42	3	0.1	162	1.5	0.2	<8	<0.1	0.2	<0.2	<0.2	0.7	4	<1	<0.1	1.5	<0.1	<0.5	<0.1	<0.1	0.5	0.22
J-47	5	0.9	215	1.6	0.2	<8	<0.1	0.4	<0.2	<0.2	0.6	3	<1	<0.1	4.0	<0.1	<0.5	<0.1	<0.1	0.5	0.22
J-52	6	<0.1	157	2.1	0.2	<8	<0.1	<0.1	0.3	<0.2	1.1	6	<1	<0.1	5.0	<0.1	<0.5	<0.1	<0.1	0.3	0.26
J-58	5	1.3	165	3.6	0.2	<8	<0.1	0.2	<0.2	0.3	0.8	5	<1	<0.1	2.3	<0.1	<0.5	0.1	<0.1	0.8	0.03
J-62	6	0.7	177	1.9	<0.1	<8	<0.1	<0.1	<0.2	<0.2	0.3	<1	<1	<0.1	1.2	<0.1	<0.5	0.2	<0.1	0.2	0.03
J-68	2	0.4	210	1.4	0.2	<8	<0.1	0.1	<0.2	<0.2	0.6	1	<1	<0.1	3.4	<0.1	<0.5	<0.1	<0.1	0.1	0.17
J-75	2	0.4	159	1.2	<0.1	<8	<0.1	<0.1	<0.2	<0.2	0.6	<1	<1	<0.1	1.4	<0.1	<0.5	<0.1	<0.1	<0.1	0.03
J-82	3	<0.1	188	1.4	<0.1	<8	<0.1	<0.1	<0.2	<0.2	0.3	<1	<1	<0.1	1.6	<0.1	<0.5	<0.1	<0.1	<0.1	0.13
J-89	5	0.3	164	1.2	<0.1	<8	<0.1	0.5	<0.2	<0.2	3.2	3	<1	<0.1	5.2	<0.1	<0.5	<0.1	<0.1	0.2	0.80
J-96	6	3.0	144	4.3	0.2	9	<0.1	<0.1	<0.2	0.3	0.5	2	<1	0.1	1.8	0.2	<0.5	0.2	<0.1	0.2	0.06
J-104	4	1.3	167	2.0	0.2	<8	<0.1	1.2	<0.2	0.2	0.6	1	<1	<0.1	0.9	<0.1	<0.5	<0.1	<0.1	0.4	0.07
J-114	2	0.5	177	1.3	0.2	<8	<0.1	1.2	<0.2	<0.2	0.4	1	<1	<0.1	2.2	<0.1	<0.5	<0.1	<0.1	0.1	0.11
J-124	3	0.8	162	1.7	0.2	<8	<0.1	0.7	<0.2	<0.2	0.6	1	<1	<0.1	0.6	<0.1	<0.5	<0.1	<0.1	0.4	0.01
J-134	2	<0.1	185	0.5	<0.1	<8	<0.1	0.3	<0.2	<0.2	0.5	<1	<1	<0.1	0.6	<0.1	<0.5	<0.1	<0.1	0.2	0.02
J-144	<1	<0.1	148	0.5	<0.1	<8	<0.1	0.8	<0.2	<0.2	0.2	<1	<1	<0.1	0.6	<0.1	<0.5	<0.1	<0.1	<0.1	0.02
J-154	2	<0.1	140	1.9	<0.1	<8	<0.1	0.4	<0.2	<0.2	0.4	2	<1	<0.1	0.5	<0.1	<0.5	<0.1	<0.1	0.2	0.02

Table 4. Rare earth element (ppm) concentrations of the Bozdağ Formation limestones

Sample	La	Ce	Pr	Nd	Sm	Eu	Gd	Tb	Dy	Y	Ho	Er	Tm	Yb	Lu	TREE	Ce/Ce*	Eu/Eu*	Pr/Pr*	La/La*	La/Sm	Dy/Sm	Y/Ho	Er/Nd	Nd/Y
J-1	2.6	1.3	0.43	2.1	0.32	0.09	0.56	0.09	0.57	8.1	0.15	0.51	0.06	0.41	0.06	9.25	0.3	0.9	1.3	2.2	1.4	1.7	54	0.24	0,5
J-4	1.6	0.7	0.21	0.9	0.15	0.04	0.23	0.04	0.31	3.4	0.06	0.17	0.02	0.15	0.02	4.60	0.2	0.9	1.4	2.0	1.9	2.0	57	0.19	0,6
J-5	4.8	3.4	0.99	4.0	0.76	0.16	0.85	0.12	0.76	6.4	0.15	0.45	0.05	0.33	0.05	16.87	0.3	0.9	1.5	1.1	1.1	1.0	43	0.11	1,1
J-8	4.0	1.5	0.67	2.9	0.53	0.13	0.69	0.09	0.59	5.2	0.13	0.33	0.04	0.22	0.04	11.86	0.2	0.9	1.6	1.6	1.3	1.1	40	0.11	1,2
J-12	4.3	2.1	0.80	3.4	0.70	0.16	0.78	0.10	0.73	6.7	0.15	0.41	0.06	0.35	0.04	14.08	0.2	0.9	1.5	1.4	1.1	1.0	45	0.12	0,9
J-17	2.2	1.1	0.37	1.5	0.34	0.07	0.43	0.06	0.38	3.9	0.09	0.29	0.03	0.21	0.03	7.10	0.3	0.8	1.5	1.4	1.1	1.1	43	0.19	0,7
J-19	5.1	2.6	1.01	4.2	0.88	0.20	1.06	0.14	0.81	7.4	0.18	0.51	0.06	0.37	0.06	17.18	0.2	0.9	1.6	1.2	1.0	0.9	41	0.12	1,1
J-24	10.3	4.2	2.08	8.9	1.68	0.37	1.95	0.27	1.66	13.8	0.36	1.03	0.13	0.80	0.11	33.84	0.2	0.9	1.6	1.3	1.1	1.0	38	0.12	1,0
J-28	8.9	6.3	2.08	8.4	1.81	0.40	2.01	0.30	1.64	13.6	0.41	1.15	0.16	0.99	0.16	34.71	0.3	0.9	1.5	1.0	0.9	0.9	33	0.14	0,8
J-32	4.0	1.3	0.77	3.2	0.58	0.16	0.90	0.13	0.85	9.9	0.19	0.63	0.07	0.48	0.07	13.33	0.2	0.9	1.7	1.3	1.2	1.4	52	0.20	0,6
J-37	7.7	2.6	1.39	6.1	1.11	0.27	1.39	0.19	1.28	14.9	0.30	0.88	0.11	0.72	0.10	24.14	0.2	0.9	1.6	1.5	1.2	1.1	50	0.14	0,8
J-42	3.6	1.8	0.73	3.2	0.62	0.16	0.83	0.11	0.78	8.1	0.18	0.50	0.07	0.43	0.06	13.07	0.2	0.9	1.5	1.3	1.0	1.2	45	0.16	0,7
J-47	2.6	1.7	0.46	1.9	0.36	0.09	0.51	0.07	0.52	4.5	0.09	0.39	0.04	0.26	0.04	9.03	0.3	0.9	1.4	1.4	1.3	1.4	50	0.20	0,7
J-52	8.4	2.1	1.48	5.8	1.31	0.32	1.69	0.24	1.59	15.4	0.33	1.05	0.13	0.76	0.12	25.32	0.1	0.9	1.8	1.2	1.1	1.2	47	0.18	0,7
J-58	4.7	2.5	0.72	3.2	0.52	0.14	0.83	0.12	0.83	12.0	0.22	0.65	0.09	0.47	0.09	15.08	0.3	0.9	1.4	1.8	1.6	1.6	55	0.20	0,6
J-62	1.6	0.7	0.21	1.0	0.22	0.04	0.27	0.04	0.23	3.3	0.05	0.20	0.02	0.16	0.02	4.76	0.2	0.7	1.3	2.6	1.3	1.0	66	0.20	0,6
J-68	1.9	1.7	0.39	1.5	0.37	0.09	0.48	0.07	0.39	3.9	0.08	0.29	0.03	0.20	0.03	7.52	0.4	0.9	1.4	1.0	0.9	1.0	49	0.19	0,7
J-75	2.0	1.3	0.37	1.5	0.31	0.07	0.41	0.06	0.40	4.0	0.09	0.27	0.03	0.22	0.03	7.06	0.3	0.8	1.5	1.3	1.1	1.3	44	0.18	0,6
J-82	1.3	0.9	0.18	0.8	0.14	0.04	0.26	0.04	0.23	2.7	0.05	0.14	0.02	0.12	0.02	4.24	0.4	0.8	1.2	2.0	1.6	1.6	54	0.17	0,6
J-89	2.1	1.2	0.39	1.8	0.34	0.09	0.51	0.07	0.46	4.8	0.09	0.29	0.04	0.23	0.03	7.64	0.3	0.9	1.4	1.7	1.1	1.3	53	0.16	0,7
J-96	4.9	3.2	1.00	4.4	0.84	0.22	1.07	0.16	0.94	8.3	0.21	0.57	0.07	0.46	0.07	18.11	0.3	1.0	1.4	1.3	1.0	1.1	40	0.13	0,9
J-104	2.6	1.5	0.47	1.8	0.41	0.10	0.51	0.07	0.51	4.4	0.09	0.29	0.04	0.25	0.04	8.68	0.3	0.9	1.6	1.2	1.1	1.2	49	0.16	0,7
J-114	1.9	1.4	0.34	1.5	0.26	0.09	0.41	0.05	0.38	3.6	0.08	0.27	0.03	0.17	0.03	6.91	0.4	1.2	1.3	1.5	1.3	1.4	45	0.18	0,8
J-124	3.6	1.9	0.58	2.4	0.53	0.13	0.76	0.11	0.70	7.7	0.17	0.49	0.07	0.42	0.07	11.93	0.3	0.9	1.5	1.5	1.2	1.3	45	0.20	0,5
J-134	2.4	1.3	0.36	1.5	0.28	0.09	0.47	0.07	0.47	5.5	0.11	0.33	0.04	0.29	0.05	7.76	0.3	1.0	1.4	1.6	1.6	1.6	50	0.22	0,48
J-144	1.7	0.9	0.24	1.1	0.24	0.06	0.31	0.04	0.31	3.9	0.07	0.21	0.02	0.18	0.02	5.40	0.3	0.9	1.3	2.2	1.3	1.3	56	0.19	0,6
J-154	1.8	0.5	0.24	1.0	0.22	0.05	0.29	0.04	0.31	4.5	0.07	0.23	0.03	0.20	0.03	5.01	0.2	0.8	1.6	1.8	1.5	1.4	64	0.23	0,5

Table 5. Redox sensitivity trace element concentrations and geochemical ratios of Bozdağ Formation limestone samples

Sample	Mo/ U	V/Cr	Ni/Co	U/Th	V/(V +Ni)	Mn/ Sr	K/ Rb	Si/ Al	Fe_T/ Al	Ti/ Al	Zr/ Nb	Zr/ Yb	Rb/ Cs	Nb/ Cr	Cr/ Ta	Cr/ Th	Nb/ U	(Rb+Cs) /La	Zr/(Nb* Ta)	(Zr*Hf)/ Nb	(Zr*Hf)/ (Nb*Ta)	Ga/ Rb	Mg/ Al	P_2O_5/ Al_2O_3	Zn/Sc	(Sr/Ca) *10^3	Al/(Ca+Mg+K+Na) *10^3
J-1	1	0.58	0.3	0.5	0.99	0.46	830	7	5.9	0.11	3	1.46	1	0.022	137	68	3	0.077	3	0.2	2	5	5.02	1	1	4.22	1.3276
J-4	1	0.58	2.3	0.5	0.92	0.56	830	7	5.9	0.11	7	4.67	1	0.007	137	68	1	0.125	7	0.7	7	5	3.42	1	2	3.49	1.3311
J-5	1	0.58	0.2	0.2	0.99	0.53	356	3.6	0.4	0.07	37	22.7	14	0.014	137	27	2	0.312	37	7.4	7.5	0.36	2.49	0.06	3	3.7	2.1471
J-8	0.25	0.58	1.3	2	0.91	0.95	830	13	8.0	0.56	11	5	1	0.007	137	68	0.25	0.050	11	1.1	1.1	5	22.19	0.5	5	4.14	0.2677
J-12	0.75	0.58	0.2	2	0.99	0.6	830	97	1.7	0.38	10	2.85	1	0.007	137	68	0.25	0.046	10	1	1	5	17.83	0.67	4	6.73	0.4117
J-17	0.25	0.58	4.0	2	0.87	0.5	830	64	2.9	0.56	8	3.81	1	0.007	137	68	0.25	0.091	8	0.8	0.8	5	19.35	0.5	3	3.96	0.2692
J-19	0.1	0.58	0.7	5	0.94	0.67	830	118	4.4	0.56	26	7	1	0.007	137	68	0.1	0.039	26	2.6	2.6	5	25.04	0.5	3	5.99	0.2730
J-24	0.5	0.58 1.09	1.9	1	0.84	1.12	246	63	0.3	0.05	41	5.12	27	0.007	137	34	0.25	0.272	41	4.1	4.1	0.18	2.33	0.09	4	10.09	3.2274
J-28	0.11		1.2	1.1	0.96	0.19	229	53	0.1	0.04	23	9.5	15	0.029	137	17	0.44	0.910	23	4.6	4.7	0.06	0.53	0.03	1	15.89	12.3573
J-32	0.5	0.58	0.3	1	0.97	1.41	830	101	5.9	0.11	14	2.91	1	0.007	137	68	0.5	0.050	14	1.4	1.4	5	3.99	3	4	7.04	1.3470
J-37	0.11	0.58	1.8	4.5	0.90	0.49	332	97	0.6	0.09	46	6.39	10	0.007	137	68	0.11	0.143	46	4.6	4.6	0.5	3.23	0.33	8	9.09	1.8017
J-42	0.5	0.58	1.0	1	0.97	0.95	830	12	1.9	0.38	15	3.49	1	0.007	137	68	0.5	0.055	15	1.5	1.5	5	11	0.33	4	4.09	0.3992
J-47	0.5	0.58	2.0	1	0.95	0.36	277	5	0.6	0.11	16	6.15	9	0.007	137	68	0.5	0.385	16	1.6	1.6	0.55	5.36	0.1	3	5.46	1.3324
J-52	0.5	0.58	0.3	1	0.99	0.99	830	8	1.2	0.23	21	2.76	1	0.007	137	68	0.5	0.024	21	2.1	2.1	5	5.94	0.4	6	3.96	0.6628
J-58	0.5	0.58	1.0	0.7	0.97	0.47	255	3	0.5	0.10	36	7.66	13	0.007	137	46	0.5	0.298	36	3.6	3.6	0.38	4.46	0.36	5	4.19	1.4665
J-62	1	0.58	0.5	0.5	0.99	0.43	237	4	0.8	0.16	9	11.9	7	0.014	137	68	2	0.500	9	0.9	0.9	0.71	5.54	0.14	1	4.48	0.9301
J-68	0.5	0.58	0.5	1	0.99	0.37	207	3	1.4	0.28	14	7	4	0.007	137	68	0.5	0.263	14	1.4	1.4	1.25	10.86	0.25	1	5.29	0.5280
J-75	1	0.58	0.5	0.5	0.99	0.48	207	3	1.4	0.28	12	5.45	4	0.007	137	68	1	0.250	12	1.2	1.2	1.25	7.71	0.25	1	3.99	0.5276
J-82	1	0.58	0.5	0.5	0.99	0.41	830	4	5.9	0.11	14	11.7	1	0.007	137	68	1	0.154	14	1.4	1.4	5	3.65	1	1	4.71	1.3182
J-89	1	0.58	2.5	0.5	0.95	0.47	277	6	1.9	0.38	12	5.22	3	0.007	137	68	1	0.190	12	1.2	1.2	1.67	9.48	0.33	3	4.11	0.3972
J-96	0.5	0.65	0.5	0.7	0.99	0.53	194	16	0.5	0.05	21	9.35	15	0.014	137	46	1	0.653	21	2.1	2.1	0.17	1.71	0.04	2	3.78	3.0318
J-104	0.5	0.58	6.0	1	0.87	0.46	191	8	0.5	0.10	20	8	13	0.007	137	68	0.5	0.538	20	2	2	0.38	3.83	0.09	1	4.25	1.4699
J-114	0.5	0.58	6.0	1	0.87	0.43	166	50	1.4	0.28	13	7.65	5	0.007	137	68	0.5	0.316	13	1.3	1.3	1	9.43	0.25	1	4.54	0.5377
J-124	0.5	0.58	3.5	1	0.92	0.47	207	2	1.0	0.16	17	4	8	0.007	137	68	0.5	0.250	17	1.7	1.7	0.62	5.38	0.14	1	4.07	0.9253
J-134	1	0.58	1.5	0.5	0.96	0.42	830	11	5.9	0.11	5	1.72	1	0.007	137	68	1	0.083	5	0.5	0.5	5	4.1	1	1	4.65	1.3221
J-144	1	0.58	4.0	0.5	0.91	0.52	830	23	5.9	0.11	5	2.78	1	0.007	137	68	1	0.118	5	0.5	0.5	5	3.19	1	1	3.71	1.3213
J-154	1	0.58	2.0	0.5	0.95	0.55	830	4	5.9	0.11	19	9.5	1	0.007	137	68	1	0.111	19	1.9	1.9	5	2.85	1	2	3.50	1.3160

Lithogeochemistry

In the Late Silurian-Middle Devonian, the Bozdağ Formation is composed of limestone deposits in the continental margin marine environment field photographsphs of the Bozdağ limestones are played in Fig. 4. The lithogeochemical results of the Bozdağ limestones are shown in Tables 2 to 5. In some examples, the concentrations of Na, Mn, and P at very low/below limit values indicate the presence of minerals such as phosphates or the adsorption of these elements on clay minerals. Some examples show relatively high concentrations of lithophile elements reflecting the pelitic-marl composition. As emphasized by Kuchenbecker et al. (2016), another feature is the low Na/K ratio, which can be directly related to the clay mineralogy.

Furthermore, the Rb/Sr ratios reflect the carbonate fraction and the relative abundance of the terrigenous content. Very low Rb/Sr ratios (0-0.02; average 0.004) in the Bozdağ limestone samples have lower values than the average upper crust value (0.32).

REE+Y shapes of the Bozdağ limestones typically show marine formation (Fig. 9a). Again, the Zr contents of the Bozdağ limestone samples show enrichment in only 5 samples (> 4 ppm, n = 27 samples, eg. Frimmel, 2009), which express a small amount of terrestrial material input during the deposition of limestones (Fig. 9b). In addition, the total rare earth element content of the Bozdağ limestones (4.2 - 34.7 ppm) is much lower than the standard North American Shale Composition (173 ppm).

Terrestrial input to the environment in which the Bozdağ limestones settled was mostly in the 30-55 m range (Fig. 6). The size of the terrestrial input particles in the Bozdağ limestone varies from clay to sand. The source of the terrestrial input in the Bozdağ limestone samples falls into the moist and arid climate zone (Fig. 9c).

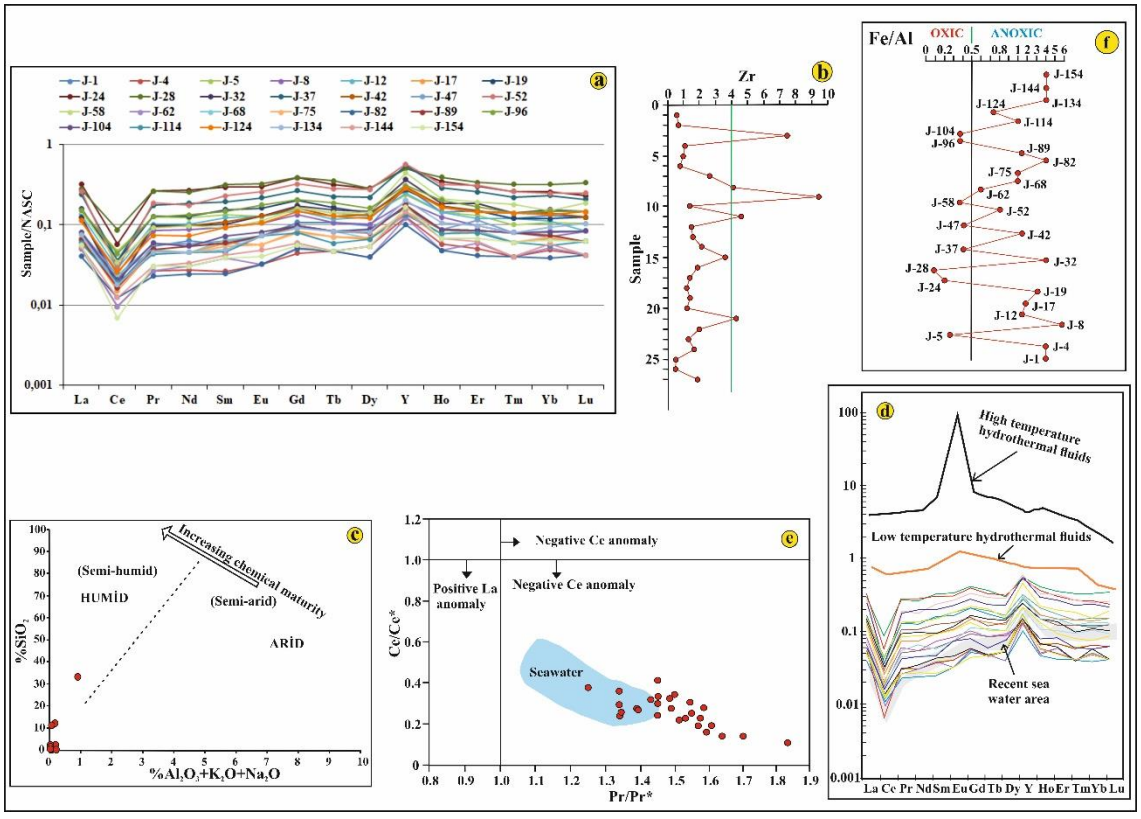

Fig. 9. a) Rare earth elements diagram normalized according to North American Shale Composition (NASC). b) Zr content of the Bozdağ limestones. c) In the diagram of SiO_2 % versus $Al_2O_3 + K_2O + Na_2O$, some of the Bozdağ limestone samples fall humid, and some of them are in the arid climate zone. d) The normalized (NASC)

REE+Y diagram of the Bozdağ limestone samples. The gray color indicates today's seawater. e) Diagram showing the relationship between Ce/Ce and Pr/Pr* for the Bozdağ limestone samples (Bau et al., 1997 method is used). All samples show positive La and negative Ce anomalies. f) Fe/Al ratio as an oxic-anoxic marker.*

Major and Trace Elements Geochemistry

The elemental and isotopic compositions of the investigeted carbonates are notified in Table 1 to 4 and demonstrated in Fig. 6. The Bozdağ limestones have SiO_2 values ranging from 0.04 to 33% (mean 2.81%), Al_2O_3 values ranging from 0 to 0.62% (average 0.08%), Fe_2O_3 values ranging from 0 to 0.11% (average 0.02%), K_2O values ranging from 0 to 0.21% (average 0.02%), TiO_2 values ranging from 0 to 0.02% (average 0.001%), P_2O_5 values ranging from 0 to 0.04% (average 0.009%), MnO values ranging from 0 to 0.05% (average 0.01%), Na_2O values 0%, CaO values ranging from 36.64 to 56.01% (average 53.94%) and MgO values ranging from 0.25 to 0.47% (average 0.35%), respectively (Table 2).

SiO_2 content of the Bozdağ limestones displays a strong positive correlation with Al_2O_3, K_2O, TiO_2, TREE, a weak positive correlation with Fe_2O_3, P_2O_5, MnO, and a strong negative correlation with CaO, but not correlated with MgO and Na_2O (Table 1).

The trace element composition of the Bozdağ Formation limestone samples is presented in Table 3. The samples of the Bozdağ limestone have Sr values between 138 and 416 (average 197 ppm), Rb values between 0 and 7.6 (average 0.83 ppm), Ba values between 0 and 45 ppm (average 8.5 ppm), Zr values between 0.5 and 9.4 ppm (average 2.3 ppm), U values between 0 and 1 ppm (average 0.2 ppm), V values between 0 and 15 ppm (average 0.9 ppm), Mo values between 0 and 0.3 ppm (average 0.02 ppm), Ni values between 0 and 1.5 ppm (average 0.5 ppm), Co values between 0 and 0.8 ppm (average 0.2 ppm), Th values between 0 and 0.8 ppm (average 0.09 ppm), Zn values between 0 and 6 ppm (average 2.5 ppm), Pb values between 0.2 and 3.2 ppm (average 0.9 ppm), Cu values between 0.5 and 17.2 ppm (average 4.4 ppm), Hf values between 0 and 0.2 ppm (average 0.02 ppm), Nb values between 0 and 0.4 ppm (average 0.05 ppm) and Cs values between 0 and 0.8 ppm (average 0.03 ppm), respectively (Table 3).

In the Bozdağ limestone samples, a strong positive correlation is observed between Rb and K_2O, and between SiO_2 and Al_2O_3 with Rb, Sr, Ba, Zr, V, Sc, Th (Table 1). Again, there is a strong positive correlation between K_2O and TiO_2 with Rb, Sr, Ba, Zr, V, Sc, Th in the Bozdağ limestone samples (Table 1). However, a strong negative correlation between CaO with Rb, Sr, Ba, Zr, V, Sc, and Th is observed (Table 1).

Mo/U, V/Cr, Ni/Co, U/Th, V/(V+Ni), and Fe_T/Al ratios are used to determine the redox conditions (eg. Taylor and McLennan, 1985; Hatch and Leventhal, 1992; Jones and Manning, 1994;) (Table 6).

Table 6. Some element concentrations used to evaluate the paleoredox conditions

Element ratio	Oxic	Dyoxic	Anoxic	Euxinic	Authors
Ni/Co	<5	5-7	>7		
V/Cr	<2	2-4.5	>4.5		Jones and Manning (1994)
U/Th	<0.75	0.75-1.25	>1.25		
V/(V+Ni)	<0.46	0.46-0.60	0.54-0.82	>0.84	Hatch and Leventhal (1992)
Fe_T/Al			>0.5		Taylor and McLennan (1985)

The Mo/U, V/Cr, Ni/Co, U/Th and V/(V+Ni) ratios of the Bozdağ limestone samples vary between 0.5 and 0.75 (average 0.05), between 0 and 1.1 (average 0.07), between 0 and 6 (average 1.6), between 0 and 1.12 (average 0.17) and between 0 and 1 (average 0.07), respectively (Table 5).

In addition, the Mn/Sr ratios of the Bozdağ Formation limestone samples are less than 3 (0 to 1.1; average 0.4), indicating that they undergo insignificant diagenetic alteration (Table 5).

The total REE+Y content of the studied limestone samples is listed in Table 4. The total rare earth element contents of the Bozdağ limestone samples are 4.24-34.71 ppm (average 12.76 ppm) and are very low compared to present-day marine sediments and North American Shale Composition (NASC). The samples of the Bozdağ limestone are normalized to North American Shale Composition (NASC; Haskin et al., 1968), rare earth elements have uniform depletion, positive La anomaly, negative Ce anomaly and remarkable positive Y anomaly (Table 4; Fig. 9a). Total rare earth element depletion is also supported by (Nd/Yb) (0.47 to 1.23; average 0.73) ratios of limestone samples (Table 4).

La_N and Ce_N anomalies were specified to show positive La and negative Ce anomalies (La/La*=0.99 to 2.61; Ce/Ce*=0.12 to 0.43; Pr/Pr*=1.24 to 1.83, respectively) by using the relationships shown in Fig. 9e. In addition, the REE+Y values normalized to the North American Shale Composition of limestone samples indicate that all samples indicate marine origin, not under the influence of any hydrothermal input, and some of them fell into the present marine environment (Fig. 9d). In addition, the samples show weak negative Eu anomaly and reasonable positive Y anomaly.

The TREE contents of the Bozdağ limestones, display a moderate positive correlation with Si, Al, Fe, K, Ti, P, Mn, Sr, Rb, Ba, Zr, Co, Sc, Th, U, Zn, and a strong negative correlation with Ca (Table 1).

Stable Isotope Geochemistry

The $\delta^{13}C$ values in the Bozdağ limestone samples ranged from 0.63 to 3.73 (average 2.5), while $\delta^{18}O$ values ranged from -9.15 to -2.12 (average -4.9) (Table 7). In addition, a very weak positive relationship was observed between $\delta^{13}C$ and $\delta^{18}O$ isotope values of the Bozdağ limestones (Fig. 10a).

In Fig. 6, the distribution of $\delta^{18}O$ and $\delta^{13}C$ isotope values of the Bozdağ limestone samples are given from the base to the top of the sequence. According to these Figs. 6 and 10, $\delta^{18}O$ and $\delta^{13}C$ isotope values in the Bozdağ limestone samples show a decrease in some levels and an increase in some levels.

There was no correlation between $\delta^{18}O$ and $\delta^{13}C$ isotope values and Mn/Sr ratios in the Bozdağ limestone samples (Fig. 10b, c). Again, between Mg/Ca ratios and Mn/Sr, $\delta^{18}O$ and $\delta^{13}C$ isotope values of the Bozdağ limestone samples were observed very weak positive, very weak negative, and very weak positive correlation, respectively (Fig. 10d-f).

The temperatures at which the Bozdağ Formation limestones were exposed during diagenetic processes were calculated with the formula by Fritz and Smith (1970) (Table 7). The O_{SMOW} isotope value of the Late Silurian-Middle Devonian sea was taken as -4 during the calculations. According to this, the temperature values of the Bozdağ limestone samples vary between 72 and 134 ^{o}C.

Table 7. $\delta^{13}C$ and $\delta^{18}O$ isotope values of the Bozdağ Formation limestone samples

Sample	$\delta^{18}O$(VPDB)	$\delta^{13}C$(VPDB)	$\delta^{18}O$(VSMOW)	Diagenesis temperature ^{o}C
J-1	-5.50	3.71	25.2	100
J-2	-9.15	2.91	21.5	134
J-3	-7.11	2.94	23.6	115
J-4	-3.83	1.94	27.0	86
J-5	-4.94	3.34	25.8	95
J-6	-3.99	2.87	26.8	87
J-8	-5.14	2.93	25.6	97
J-9	-4.02	3.09	26.8	87
J-10	-2.27	3.33	28.6	73
J-11	-8.02	1.94	22.6	123
J-12	-6.67	2.74	24.0	110
J-13	-2.71	2.45	28.1	77
J-14	-4.23	3.73	26.5	89
J-15	-2.91	1.92	27.9	78
J-17	-3.56	1.20	27.2	84
J-19	-3.59	1.90	27.2	84
J-21	-2.12	3.04	28.7	72
J-24	-5.81	2.58	24.9	103
J-28	-7.66	1.32	23.0	120
J-32	-2.80	2.81	28.0	78
J-37	-6.76	0.63	23.9	111
J-42	-5.49	1.69	25.3	100
J-47	-3.20	2.66	27.6	81
J-52	-5.49	2.71	25.3	100
J-58	-5.00	3.17	25.8	96
J-62	-4.35	2.36	26.4	90
J-68	-5.55	2.86	25.2	100
J-75	-6.00	2.78	24.7	104
J-82	-5.25	1.99	25.5	98
J-89	-5.71	2.12	25.0	102
J-96	-5.39	2.48	25.3	99
J-104	-4.49	2.11	26.3	91
J-114	-5.21	2.62	25.5	97
J-124	-4.34	2.09	26.4	90
J-134	-3.89	2.65	26.9	86
J-144	-5.10	2.00	25.6	96
J-154	-2.88	3.17	27.9	78

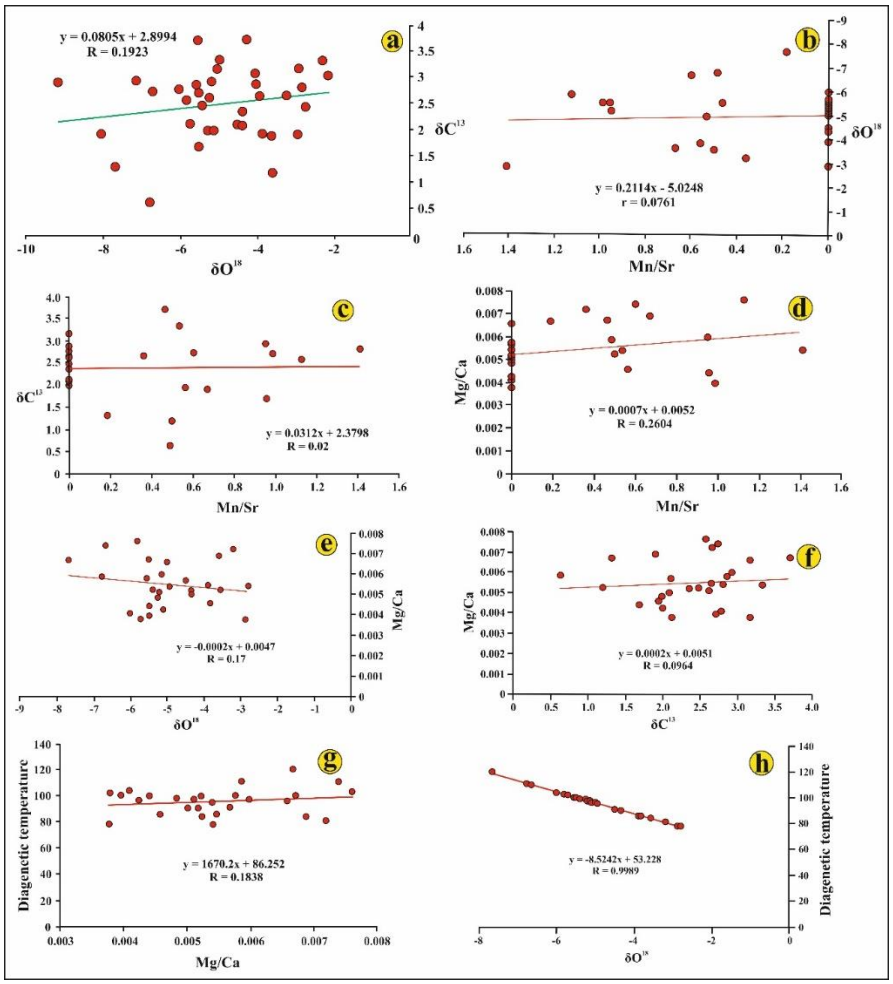

Figure 10. a) diagram of $\delta^{13}C$ versus $\delta^{18}O$ of the Bozdağ limestone samples, b) the relationship between $\delta^{18}O$ and Mn/Sr of the Bozdağ limestone samples, c) the relationship between $\delta^{13}C$ and Mn/Sr of the Bozdağ limestone samples, d) the relationship between Mn/Sr and Mg/Ca of the Bozdağ limestone samples, e) the relationship between Mg/Ca and $\delta^{18}O$ of the Bozdağ limestone samples, f) the relationship between Mg/Ca and $\delta^{13}C$ of the Bozdağ limestone samples, g) the relation between Mg/Ca and diagenetic temperature (°C) values of the Bozdağ limestone samples, h) the relationship between $\delta^{18}O$ isotope and diagenetic temperature (°C) values of the Bozdağ limestone samples.

A very weak positive correlation is observed between the Mg/Ca ratios and the diagenetic temperature values of our samples (Fig. 10g). Considering the change in the ratio of the Mg/Ca and diagenetic process temperature values from the base to the top of the sequence, it is seen that these values offer fluctuation, that is, the decrease-increase states repeat many times. The relationship between diagenetic temperatures and δC and δO isotope values of the Bozdağ Formation limestone samples was investigated and a very strong negative relationship was found between the temperature and the δO isotope values (R=-0.98), that is, while the temperature increases, δO isotope values decrease; It was found that there was no relationship between temperature and δC isotope values, ie temperature increase did not affect δC isotope values (Figs. 10h, 11a-c). Therefore, δC isotope ratios are not affected by diagenetic temperatures and they can be used in chemical stratigraphic studies. However, δO isotope values have the possibility of losing their original composition due to diagenetic alteration, and therefore should be used carefully in chemical stratigraphic studies.

Furthermore, there is a very low correlation or no correlation between $\delta^{13}C$ and $\delta^{18}O$, Sr, Fe, Mn, and Mn/Sr (Figs. 11d-f, 10b,c). Again, a weak negative correlation is observed between $\delta^{18}O$ and Sr and Fe (Fig. 11g,h).

Joachimski et al. (2009) stated the oxygen isotope composition of surface waters in epeiric seas may be influenced by higher evaporation or enhanced freshwater input. Whereas enhanced evaporation will result in higher salinities and $\delta^{18}O$ values, freshwater input will lower the salinity and $\delta^{18}O$ of surface waters. Late Silurian-Middle Devonian temperatures are 32°C and 22°C, respectively, on average at 27°C (Joachimski et al., 2009). Calculated temperature values using $\delta^{18}O$ values of the Bozdağ limestones yield precipitation temperatures of 72 to 134°C, and suggest burial depths of 1500 to 3500 m, i.e., they express intermediate to deep burial (assuming a normal geothermal gradient 30 km^{-1}).

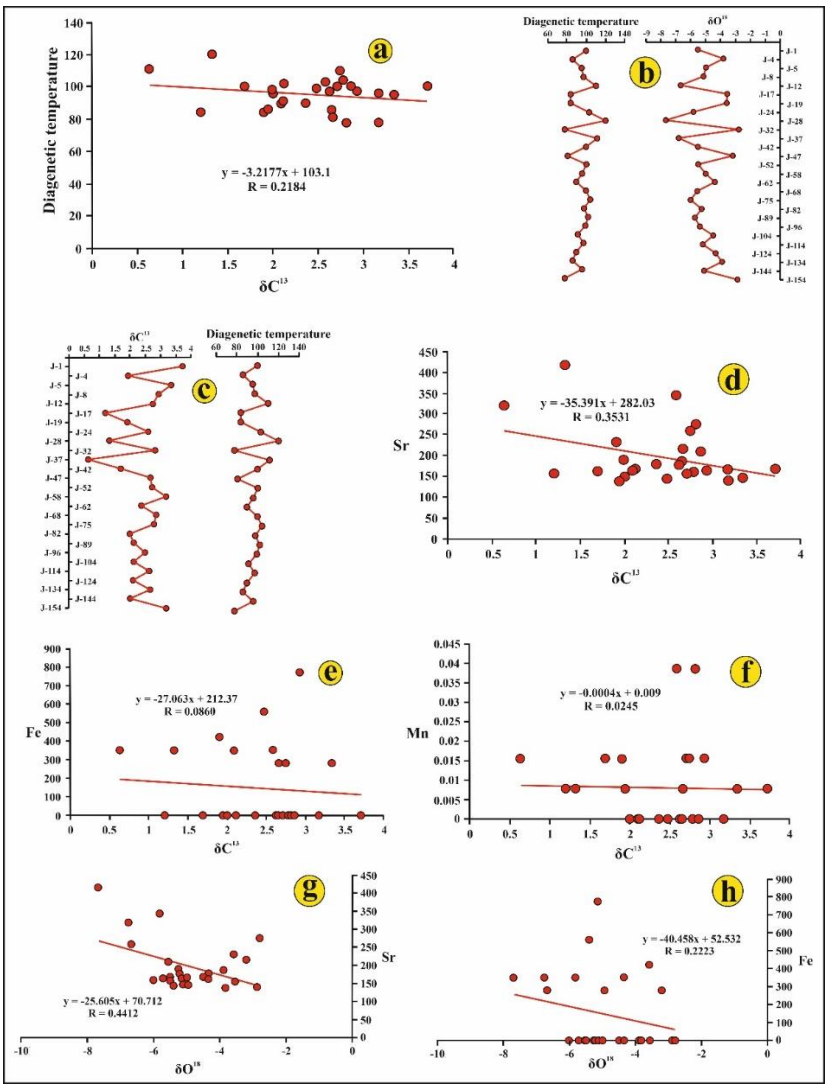

Figure 11. a) the relationship between $\delta^{13}C$ isotope and diagenetic temperature (°C) values of the Bozdağ limestone samples, b) the opposite relationship between $\delta^{18}O$ isotope and diagenetic temperature (°C) values of the Bozdağ limestone samples, c) there is no relation between $\delta^{13}C$ isotope and diagenetic temperature (°C) values of the Bozdağ limestone samples along the sequence, d) the relation between $\delta^{13}C$ and Sr of limestone samples of Bozdağ Formation, e) the relation between $\delta^{13}C$ and Fe of limestone samples of Bozdağ Formation, f) the relation between $\delta^{13}C$ and Mn of limestone samples of Bozdağ Formation, g) the relation between $\delta^{18}O$ and Sr of limestone samples of Bozdağ Formation, h) the relation between $\delta^{18}O$ and Fe of limestone samples of Bozdağ Formation.

Discussion

Evaluation of Sample Protection

In geochemical studies, the degree of protection of the textural and chemical properties of the samples to be analyzed is very important. The process of diagenesis may cause some elements to enrich and some to become poor. Besides, diagenesis has a change effect on stable $\delta^{18}O$ and $\delta^{13}C$ isotope values. Therefore, it is important to determine the degree of variation of the collected samples during the diagenesis before the transition to the geochemistry of the carbonate rocks. Some tests should be performed to determine the degree of this change.

As Brand and Veizer (1980) state, textural change in carbonate rocks may occur as a result of the transformation of unstable minerals into more stable minerals (Wang et al., 2017). During diagenesis, micritic and/or sparrytic calcite can be transformed into larger sparrytic calcite by neomorphism. In all of the Bozdağ limestone samples, it was observed that the limestones, which were initially micritically deposited, were largely microsparrytic and to a lesser extent sparrytic limestone. However, we must state that micritic texture is preserved to a small extent in some samples.

Elemental ions such as Sr, Mg, Fe, and Mn can participate in carbonate minerals. Meteoric waters have low Sr^{2+}, but high Fe^{2+} and Mn^{2+} contents (Brand and Veizer, 1980; Wang et al., 2017). The $\delta^{18}O$ and $\delta^{13}C$ isotope values in the meteoric waters are more negative than the $\delta^{18}O$ and $\delta^{13}C$ isotope values of seawater. Therefore, while the diagenetic process causes enrichment in Fe^{+2} and Mn^{+2} content, it will cause depletion in Sr^{+2}, $\delta^{18}O$ ve $\delta^{13}C$ content. In contrast, Mg^{+2} content may increase or decrease depending on the original carbonate mineral (Brand and Veizer, 1980; Wang et al., 2017). So, as Wang et al. (2017) emphasized, changes in trace elements are important markers because they can reflect the degree of diagenesis and carbonate alteration after sedimentation.

Furthermore, because our samples have low Mn/Sr ratios, may, therefore, reject the possibility of diagenetic alteration in the Bozdağ limestone samples. Again, low Mg/Ca ratios in the Bozdağ limestones further exclude the possibility of dolomitization. A non-linear correlation between Mn/Sr and Mg/Ca further excludes the probability of metamorphic dolomitization in the Bozdağ samples (Fig. 10d).

The elements Sr and Mn are sensitive elements of post-deposition diagenesis (Wang et al., 2017). While Sr^{2+} is easily removed from the carbonate lattice by meteoric diagenesis, Mn^{2+} can be easily absorbed from the diagenetic water into the carbonate lattice during post-deposition diagenesis (Brand and Veizer, 1980; Wang et al., 2017).

The Mn/Sr ratio of the Bozdağ limestone samples changed from 0.2 to 1.4 (average 0.4), and the isotope values retained their original seawater characteristics. Therefore, the $\delta^{18}O$ and $\delta^{13}C$ isotope values of the Bozdağ limestone samples can be used in geochemical interpretations.

The $\delta^{18}O$ isotope values of the Bozdağ limestone samples show a sudden rise and fall in some levels from the base to the top of the sequence. This may suggest, in the mesodiagenetic process, in the middle and upper levels of the sequence, possibly in areas with high effective porosity, under the influence of geothermal or hydrothermal fluids or under the influence of meteoric waters during telodiagenesis. However, $\delta^{13}C$ isotope values of carbonates affected by meteoric waters are negative. Therefore, the $\delta^{13}C$ isotope values of the Bozdağ limestone samples are positive and suggest that there is no meteoric water diagenesis. In addition, the $\delta^{18}O$ isotope values are more sensitive to temperature, thus reaching more negative values as the temperature increases (burial/hydrothermal). Hydrothermal effects show positive Eu and high Ba values. However, the weak negative Eu (Fig. 9a,d) and low Ba values are observed in the Bozdağ limestone samples. In particular, even at levels that have very low $\delta^{18}O$ isotope values, low Ba is observed (Tables 9 and 2). In addition, any hydrothermal effect is not observed in our samples in Fig. 9d. Again, in our Y/Ho-Eu/Sm diagram (Fig. 12a), it is observed that our samples retain their original seawater

characteristics and do not remain under the influence of hydrothermal water. Therefore, we can say that there is a geothermal fluid effect caused by the increase in temperature due to burial.

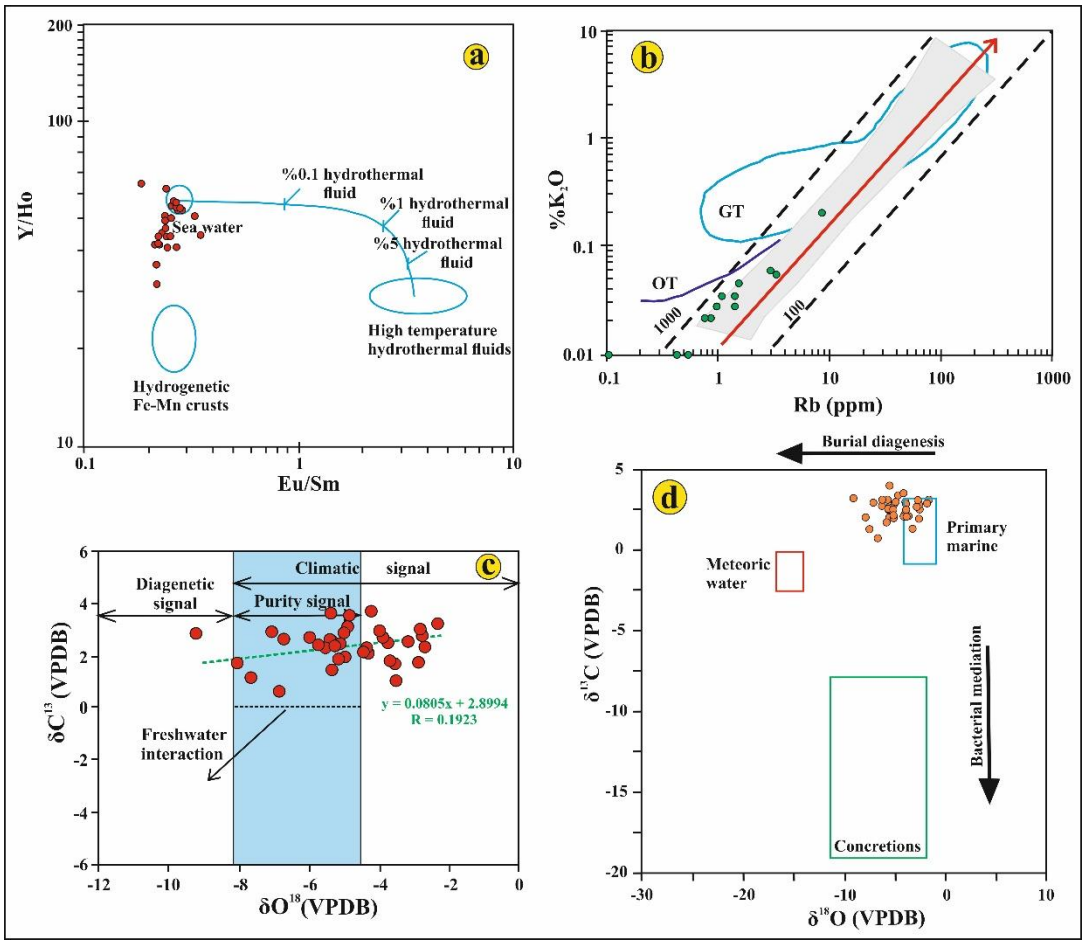

Figure 12. a) Diagram of Y/Ho versus Eu/Sm. Samples retained seawater characteristics. b) The location of Bozdağ limestone samples on the K_2O-Rb diagram. OT: the trend of granite on the ridge of the ocean, GT: GT: granule trend. The gray-colored zone is a magmatic rock trend (after Rudnick et al., 1985; Maity and Indares, 2018). c) The position of the Bozdağ limestone samples on the very weak positive correlation $\delta^{13}C$ versus $\delta^{18}O$ diagram (Diagram is taken from Salama et al., 2016). No meteoric water interaction is observed in the samples, very little diagenetic effect, protection of primary properties, and significant climatic effects are observed in nearly all samples. d) $\delta^{18}O$-$\delta^{13}C$ cross plot of all data from this study, the diagram is taken from Nakamura (2015).

Ce anomaly values in the Bozdağ limestone samples changed from 0.13 to 0.43 (average 0.27; n = 27). As some researchers (eg, Elderfield and Greaves, 1982; Piepgras and Jacobsen, 1992) emphasized, the Ce/Ce* ratios change from <0.1 to 0.4 in oceanic water. In the average shale, the ratio of Ce/Ce* is around 1 (Murray et al., 1991). In addition, the $(La/Sm)_N$ ratio in all samples of the Bozdağ limestones is >0.87, and the lack of correlation between Ce anomaly and La/Sm (R = -0.06), as Chen et al. (2012) emphasized, shows that there is no effect of diagenesis on true Ce anomaly values. Therefore, negative Ce anomalies of the Bozdağ limestone samples display oceanic water characteristics.

Rudnick et al. (1985) and Bauernhofer et al. (2009) emphasized that the K/Rb ratios of the high-grade metamorphic rocks are higher (ie, ≥500 in the granite facies), that the non-metamorphic igneous rocks 230 (except for the oceanic tholeiites) and the shales have 200 K/Rb ratios. The

K/Rb ratios of the Bozdağ limestone samples (0.0083 to 0.083) are quite low and do not show any metamorphism effect. Although K and Rb are thought to be mobile during transport, diagenesis, and metamorphism, many investigators (eg, El-Bialy, 2013) have been found to be effective and relatively uniform in their determination of source rocks. Furthermore, in the K_2O-Rb diagram presented in Fig. 12b, the Bozdağ limestone samples are mostly located in the region of the trend of magmatic rocks; the Bozdağ limestone samples retain their primary sedimentary rock properties, ie they are not affected by metamorphism, but only by diagenetic processes. Therefore, it is seen that the primary geochemical characteristics of the Bozdağ limestones are largely preserved and the unit can be used in the interpretation of paleo-environmental conditions and in the study of geochemistry.

The $\delta^{13}C$ values of the Bozdağ limestone samples were not negative, and they were positive values, indicating that they are not exposed to any atmospheric exposure and meteoric water effects (Fig. 12c,d). In addition, no correlation was observed between the $\delta^{18}O$ and $\delta^{13}C$ isotope values and Mn/Sr ratios in the Bozdağ limestone samples (Fig. 10b,c), and it displays limestone samples maintain their original values and do not undergo any significant alteration due to diagenesis. Again, in the Bozdağ Formation limestone samples, between Mg/Ca ratios and Mn/Sr, $\delta^{18}O$, $\delta^{13}C$ isotope values were very weak positive, very weak negative, and very weak positive relation, respectively (Fig. 10d-f). It shows that the Bozdağ limestones do not undergo a significant alteration and therefore retain their original properties.

The carbon reserve in water is much smaller than that of oxygen, and much higher water/rock ratios are required to significantly reduce the $\delta^{13}C$ values of limestones (Armstrong-Altrin et al., 2009). The change due to this water/rock ratio is very insignificant in the $\delta^{13}C$ and $\delta^{18}O$ values of the Bozdağ limestones (Fig. 12c,d).

Major, Trace, and Rare Earth Element Evaluation of The Bozdağ Formation Limestones

The behavior of trace elements during sedimentary processes is complex depending on factors such as decomposition, physical sizing, adsorption, provenance, diagnosis, and metamorphism (eg, Taylor and McLennan, 1985; Wronkiewicz and Condie, 1987). The major and trace element patterns in the carbonate rocks are strongly influenced by the terrigenous content (Kuchenbecker et al., 2016). Si, K, Al, Ti, and other lithophile elements (Rb, Sr, Ba, Nb, Ta, Th, U, REE) in the Bozdağ limestone are generally at low ratios, although they are observed at high ratios in some stages of the terrigenous input.

Zhang et al. (2017) emphasized that Ca is predominantly biogenic and is essentially a diluent of all other components, as evidenced by strong negative correlations with all other major and trace elements (Table 1). The content of Al_2O_3 shows no correlation with MnO (R=0.07) in the Bozdağ limestones, but it shows a positive correlation with Fe_2O_3 (R=0.44), which indicates that at least Fe_2O_3 is partly controlled by clay minerals. Again, the strong positive correlations between TiO_2 and K_2O (R=0.91), K_2O and Al_2O_3 (R=0,99), and TiO_2 and Al_2O_3 (R=0.91) in the Bozdağ limestone samples (Table 1) indicate that TiO_2 and K_2O were mainly from aluminosilicate clastics (clays). Almost all other major elements, except CaO and MgO in the Bozdağ limestones, show a good positive correlation with each other (Table 1).

Kuchenbecker et al. (2016) reported that the Rb/Sr ratios reflect the terrigenous content and the relative abundance of the carbonate fraction. The Rb/Sr ratios of the Bozdağ limestone samples ranged from 0 to 0.018 (average 0.004), it is slightly above (falling to 0.0008; Kuchenbecker et al., 2016) the expected very low rate in carbonates (14/27 examples this reflects the 0.0008 rates) and reflects a small amount of Sr loss in the diagenetic process. The low content of the trace element content of the Bozdağ limestone samples indicates that the terrigenous input is a small proportion during deposition.

Th/U ratios are also used as a useful indicator in determining the source of the contaminations in sediments of chemical origin. Sediments of chemical origin may sometimes contain detrital materials such as volcanic ash, detritic material, and phosphate, whose origins cannot be determined (Thurston et al., 2011). Phosphate contamination is generally characterized by the Th/U>5 ratios (Thurston et al., 2011), while the other contaminations are characterized by the Th/U ratio between 3 and 5 (Thurston et al., 2011). Th/U ratios in the Bozdağ limestones vary between 0.2 and 5 (average 1.4), so there is no phosphate contamination in our samples, but there is some terrigenous contamination.

As the total Fe_2O_3 content increases, the weakening of Eu anomalies indicates that iron is predominantly of terrigenous origin and the negative Eu anomaly intensity decreases with the increase of the input of the terrigenous material (Frimmel, 2009).

Correlations between Al_2O_3 with immobile trace elements Zr (R=0.9) and Th (R=0.9) of the Bozdağ limestone samples demonstrate a strong positive relationship (eg, Nothdurft et al., 2004), suggesting that these elements are terrigenous origin (Table 1). In addition, Song et al. (2014) stated that the strong positive correlation between REE and Zr, and REE and Th in limestones represent terrestrial clastic contamination. In the Bozdağ limestone samples, the strong positive correlation between REE and Zr (R=0.7) and REE and Th (R=0.7) shows that REE of the Bozdağ limestone is affected by detritus (Table 1).

Bau and Dulski (1996) expressed that precipitation of oxidized cerium (CeO_2) as absorbed by Mn- and Fe-oxy-hydroxides, seawater, and chemical sediments deposited from this water displayed negative Ce-anomaly, and Fe and Mn-rich sediments at the bottom will show positive Ce anomaly values.

The correlations of Al_2O_3 with Fe_2O_3 and MnO of the Bozdağ limestone samples were R=0.65 and R=0.24, respectively; it states that although Fe and Mn originate mainly from marine waters, they are partly due to clays.

Previous research suggests that the distribution and relative content of some major and trace elements in fine-grained rocks may reveal paleoclimatic conditions (Cao et al., 2012; Wang et al., 2017; Ding et al., 2018). A consensus was reached by previous studies that Fe, Mn, V, Cr, Co, and Ni were relatively enriched under humid climatic conditions (Cao et al., 2012; Wang et al., 2017; Ding et al., 2018). On the contrary, the increase in water alkalinity due to evaporation under dry climatic conditions facilitates the deposition of salty minerals, in this way, elements such as Ca, Mg, Na, K, Ba, and Sr are relatively concentrated (Ding et al., 2018). In view of the different geochemical behaviors of these two groups, $\Sigma(Fe+Mn+Cr+Ni+V+Co)/\Sigma(Ca+Mg+Sr+Ba+K+Na)$ ratios (named C-value) are accepted as a climate indicator, and it has been widely applied in the interpretation of Paleoclimate (Cao et al., 2012; Wang et al., 2017). Numerous investigators (eg, Ding et al., 2018) concluded to show 0 to 0.2, 0.2 to 0.4, 0.4 to 0.6, 0.6 to 0.8, 0.8 to 1 C-values arid, semiarid, semiarid to the semihumid, semihumid and humid climate, respectively. C-values of the Bozdağ limestone samples are <<0.2, and they demonstrate an arid climate.

In addition, some trace element ratios, such as Sr/Cu and Ga/Rb ratios, can also be used to characterize the paleo-climate (Roy and Roser, 2013; Xie et al., 2018; Ding et al., 2018). Ga is mainly enriched in clay minerals, especially kaolinite, and warm, and humid express climatic conditions (Roy and Roser, 2013; Ding et al., 2018). Rb is closely related to illite and reflects the cold and arid climate (Roy and Roser, 2013; Ding et al., 2018). The more cold and dry the climate, the lower the Ga/Rb ratios in the sediments. Generally, fine-grained sediments are characterized by low Sr/Cu ratios and high Ga/Rb ratios in warm and humid climatic conditions (Cao et al., 2012; Xie et al., 2018; Ding et al., 2018). The values of Sr/Cu between 1.3 and 5.0 may indicate warm humid environments, while values above 5.0 indicate hot-arid climatic conditions (Cao et al., 2012; Ding et al., 2018). Therefore, the Sr/Cu values of the Bozdağ limestone samples vary between 20 and 308 (average 110) indicating hot-arid climatic conditions.

The enrichment and depletion of REE in limestones may be affected by various factors, for example, (1) the addition of terrigenous particles from the continent (McLennan, 1989), (2) biogenic precipitation from the upper seawater (Murphy and Dymond, 1984) and (3) depth, salinity and oxygen levels to related effect (Elderfield, 1988; Greaves et al., 1999), (4) removal of REE from the water column and autogenously early diagenesis (Sholkovitz, 1988).

Seawater contributes a lower amount of REE to chemical sediments, but not sea water-like examples, exhibit higher REE concentration due to contamination (Nothdurft et al., 2004) non-carbonate materials such as silicates, Fe-Mn oxides, phosphates, and sulfides during chemical leaching (Zhao et al., 2009). The Bozdağ limestone samples are marine in nature and contain low amounts of REE and support this view.

Zhang et al. (2017) stated that TREEs in terrestrial and marginal limestones show a clear positive correlation with SiO_2, Al_2O_3, TiO_2, and Fe_2O_3 (R=0.79, 0.48, 0.67, 0.45, respectively), indicating the control of the detrital siliciclastic fraction on REE. A good positive correlation was observed in TREE of the Bozdağ limestone samples with SiO_2 (R=0.88), Al_2O_3 (R=0.85), TiO_2 (R=0.58), Fe_2O_3 (R=0.72), K_2O (R=0.86) (Table 1) also shows that there is control of detrital siliciclastics on REE.

Analog to the alteration tendency of Ce anomalies (Ce/Ce*) monitored in waters and cherts as well as fine-grained marine sediments, the greatness of the Ce anomalies of the limestones displays a prominent increment from spreading ridge to the continental coastal sea (Zhang et al., 2017). In the diagram of the Ce/Ce* anomaly of the Bozdağ limestone samples versus Al_2O_3, Fe_2O_3, and MnO, all samples fall into the open sea environment in terms of deposition environment (Fig. 13a-c).

The Er/Nd ratio in normal seawater is approximately 0.27 (De Baar et al., 1988; Song et al., 2014). The high Er/Nd ratio of limestone effectively demonstrates the protection of the seawater marker by marine carbonate (Song et al., 2014). In addition, Bellanca et al. (1997) and Song et al. (2014) emphasized that detrital material or diagenesis may reduce the Er/Nd value to less than 0.1 for the preferential concentration of Nd relative to Er. The Er/Nd ratios of the Bozdağ limestones ranged from 0.11 to 0.24 and a high positive correlation between Nd and Er (R=0.95) was observed (Fig. 13d), it is another indicator that shows the effect of detrital material on these limestones.

Diagenesis will change the values of Ce and Eu anomalies together with good correlations between Ce/Ce* and TREE and between Ce/Ce* and Eu/Eu* (Song et al., 2014). However, as shown in Fig. 13d,e, there was no significant correlation between Ce/Ce* and TREE and between Ce/Ce* and Eu/Eu* in the Bozdağ limestones, or a weak correlation (R=-0.33 and R=+0.17, respectively), that indicates the effect of the diagenesis process on REE concentrations are very limited.

All rock Ce anomaly with a positive tendency shows more oxic conditions or sea-level fall (Wilde et al., 1996; Chen et al., 2012). On the other hand, Ce anomaly with a negative tendency refers to more reducing conditions or sea-level rise.

As the sedimentary environment of the Bozdağ Formation limestones (reefal complex) is a transgressive, shallow marine environment (carbonate-dominated shelf), Wilde et al. (1996) suggest that the model is applicable in this study. Therefore, the Ce values of the Bozdağ limestone samples (in our study, it was determined that the values of Ce were true) the transgressive carbonate precipitation, ie the precipitation in the anoxic environment rather than the oxic environment (except for some short-term stages), since these are true negative values (Fig. 9e).

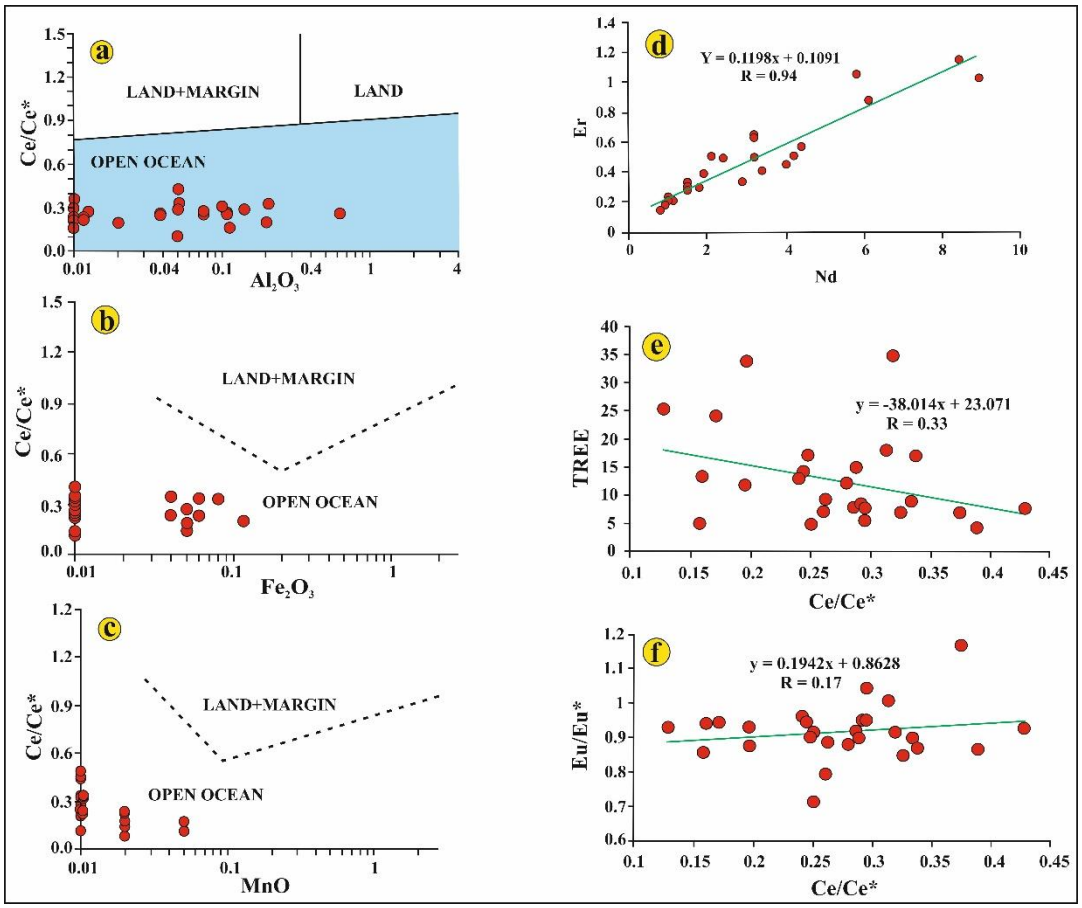

Figure 13. a-c) Diagram of Ce/Ce anomaly of the Bozdağ limestone samples versus Al_2O_3, Fe_2O_3, and MnO. Limestones are deposited in various sedimentation environments (Taylor and McLennan, 1985). d) Diagram of Er versus Nd. e) Diagram of Ce/Ce* anomaly of the Bozdağ limestone samples versus TREE and f) Diagram of Ce/Ce* anomaly of the Bozdağ limestone samples versus Eu/Eu*.*

Zhang et al. (2017) emphasized that Ce concentrations in marine limestone have a strong positive correlation with Al_2O_3, Fe_2O_3, and MnO, and Ce anomalies show a positive correlation with Al_2O_3 and MnO, which indicates both terrigenous and metalliferous input in these rocks. The Ce concentrations of the Bozdağ limestones, are strongly positively correlated with Al_2O_3, SiO_2 ve K_2O, and the Ce anomalies are moderately positively correlated with Fe_2O_3, and weakly positively correlated with MnO, and their Ce anomalies are weakly positively correlated with Al_2O_3 ve K_2O, and the Ce anomalies are weakly negatively correlated with Fe_2O_3, MnO ve SiO_2 (Table 1). It states that during the deposition of limestones there is some terrigenous input. In addition, there were no hydrothermal effects in the Bozdağ limestone samples were determined in Figs. 9d and 12a, and non-positive Eu (Fig. 9a) anomaly and low Ba (Table 3) values. Furthermore, in the Bozdağ limestones, the positive correlation between Ce anomaly and Fe_2O_3 and MnO showed that there was no hydrothermal effect; because Abedini and Calagari (2015) reported a negative correlation between Ce anomaly and Fe_2O_3 and MnO, indicating the hydrothermal effect.

Ali and Wagreich (2017) reported that Ce anomalies in the limestones of Mannersdorf and Wöllersdorfde were close to 1 and therefore different from seawater values (0.1 to 0.4). This situation can be explained in two ways, (1) the presence of small amounts of clay (detritic input) minerals in pure and impure samples, (2) a few cm deep of the sediment column below the seafloor, it may be due to the increase of LREEs due to degradation of organic matter containing Ce. Ce anomaly values in the Bozdağ limestone samples change between 0.13 and 0.42 (average 0.27) and

are consistent with seawater values. The fact that the Ce anomaly values of our samples are consistent with seawater shows that there is little or no detrital input to the deposition in an anoxic environment.

However, the fact that our samples have fallen into the oxic area in the Y/Ho versus Pr/Pr* contrasts with this situation. Therefore, during the Bozdağ limestone precipitation, it suggests that the oxic and anoxic conditions are repeated. Already, during the Late Silurian-Middle Devonian process, it is known that there are fluctuations at sea level, and we can say that there is no discrepancy between these two results.

Seawater usually has high Y/Ho ratios (~44 to 74), while the terrigenous materials and volcanic ash have a constant chondritic Y/Ho ratio of ~28. Today's seawater has significantly higher Y/Ho ratios than river water and estuaries (Lawrence et al., 2006). Y/Ho ratios show a significant difference between open seawater and ocean margin seawater between 108 and 94, respectively (Johannesson et al., 2006).

The Y/Ho ratios of the Bozdağ Formation limestones (Table 4) show a lower average value of 48 compared to the open seawater standard (60-90). This indicates that freshwater suspended load and/or wind-blown powders are effectively mixed during the deposition of the Bozdağ limestones (eg, Kuchenbecker et al., 2016). In addition, Y/Ho values of the Bozdağ limestone samples vary between 33 and 66 and are described in Song et al. (2014), while maintaining a large proportion of seawater ratios (excluding 7 samples, n: 27), which implies a certain amount of terrestrial input and some fluctuations in the seawater level.

Oxygen and Carbon Isotope Evaluation of The Bozdağ Formation Limestones

All Bozdağ limestone samples show positive $\delta^{13}C$ values (0.63 to 3.73 ‰; Table 7, Figs. 6 and 12c,d). These C-isotope values are Hudson (1977), and Armstrong-Altrin et al. (2009), as emphasized, are consistent with the $\delta^{13}C$ values (0 to 4‰) of today's marine carbonates.

Carbon isotopes are less affected by diagenesis than oxygen isotopes (Madhavaraju et al., 2017). In addition, the strong positive correlation observed between carbon and oxygen isotope values is an indicator of diagenetic alteration (Madhavaraju et al., 2017). A very weak positive relationship (R = 0.036) is observed between the oxygen and carbon isotope values of the Bozdağ limestones. This displays that the carbon isotope values of our samples are not affected an important by diagenesis (Fig. 12c). In addition, no correlation was observed between the $\delta^{18}O$ and $\delta^{13}C$ isotope values and Mn/Sr ratios in the Bozdağ limestone samples (Fig. 10b,c), and it displays limestone samples maintain their original values and do not undergo any significant alteration due to diagenesis. Again, in the Bozdağ Formation limestone samples, between Mg/Ca ratios and Mn/Sr, $\delta^{18}O$, $\delta^{13}C$ isotope values were very weak positive, very weak negative, and very weak positive relation, respectively (Fig. 10d-f). It shows that the limestones do not undergo a significant alteration and therefore retain their original properties.

Considering the change in the ratio of Mg/Ca and diagenetic process temperature values from the base to the roof of the sequence, these values present fluctuation, that is, situations of the reduction and increment can be seen repeated several times (Fig. 10g). In this case, we think, the increase in temperature is caused by the increase in temperature due to burial, and the increase in Mg is probably due to the transformation of clay minerals (smectite to illite transformation).

The $\delta^{18}O$ of diagenetic carbonate phases are primarily checked up by fluid composition, temperature, and water/rock ratios (Brand and Veizer, 1981; Hajikazemi et al., 2010), and accordingly the $\delta^{18}O$ values are anticipated to be reset by diagenetic alteration. According to Al-Aasm and Veizer (1986), meteoric diagenesis of marine carbonates typically ends up in a slip toward more negative values of both $\delta^{13}C$ and $\delta^{18}O$. However, since the carbon isotope values of all our samples are positive, we cannot speak of a meteoric diagenesis effect (Table 7, Fig. 12c,d).

The Bozdağ limestones from the entire section show distinct negative oxygen isotope values (-9.15 to -2.12‰ VPDB; Table 7; Figs. 10a and 12c,d). Thus, some of our examples (15, n: 36, Fig. 12d) are consistent with marine environment values, while others represent burial diagenetic alteration. The Late Silurian $\delta^{18}O_{SMOW}$ ranged from 16.2 to 19.2 (van Geldern et al., 2006). Early Devonian $\delta^{18}O_{SMOW}$ ranged from 16.3 to 21, while Middle Devonian $\delta^{18}O_{SMOW}$ ranged from 17.8 to 21.3 (van Geldern et al., 2006). $\delta^{18}O_{SMOW}$ values of the Bozdağ limestone samples vary between 21.5 and 28.7. Therefore, $\delta^{18}O_{SMOW}$ values of the Bozdağ limestone samples emphasize diagenetic alteration (Table 7).

In the case of interacting with isotopically heavy fluids (eg, evaporitic saline, conventional rising water), there will be an increase in $\delta^{18}O$ values (Kuchenbecker et al., 2016). From here, we can say that the fluctuations of $\delta^{18}O$ values in the Bozdağ limestone samples (Fig. 6), it may be caused by the effects of isotopic heavy and light fluids.

Kuchenbecker et al. (2016) stated that the strong negative decrease in $\delta^{13}C$ values corresponded to a period of intensive reduction in biological activity. Researchers have stated that the increase in later $\delta^{13}C$ values shows that biological activity is increasing gradually and it shows the restoration of atmosphere/sea interaction. The $\delta^{13}C$ values observed in the Bozdağ limestone samples are all positive and show little fluctuation in the values (base of the sequence: 0-85 m); there is no significant change in the biological productivity of the Late Silurian-Middle Devonian Sea; it is thought that the positive decreases and increases in the values (at least a large part) are due to the input of the wind-blown sediments. The relatively stable $\delta^{13}C$ values (slightly fluctuation) in the middle and upper part (85 to 265 m) of the sequence indicate both stable environment conditions (light, temperature, etc.) and a stable period of bio-productivity.

At some levels of the Bozdağ Formation, limestones with *Amphipora* (Özkan, 2016), stromatoporoid bioherms (Fig. 4e), and coral reefs (Eren, 1996), observed the positive increase in $\delta^{13}C$ values suggests that it may be due to the increase in bio-productivity and, less the changes during burial.

It can also be thought that positive $\delta^{13}C$ isotope deviations can be followed by an increase in $\delta^{18}O$ values (Kuchenbecker et al., 2016). Therefore, when we apply this view to the limestones of the Bozdağ Formation, the positive deviations in $\delta^{13}C$ values as seen in Figs. 10a,b, and 12a,b, increases in $\delta^{18}O$ values support this view.

The difference between the examples in Fig. 12c should probably be due to the diagenetic effect or climatic and paleoenvironmental changes. No significant correlation was observed between $\delta^{18}O$ and $\delta^{13}C$ (Fig. 10a), indicating that the diagenetic effect was not significant in our samples. However, the fact that almost all of our samples fall into the climatic change area suggests that the changes in paleoenvironmental conditions are effective in our samples. These comments are consistent with the results in the elemental section.

Fluctuations in the isotope values of the Bozdağ Formation (Fig. 6), as Salama et al. (2016) emphasizes, it is probably due to the siliciclastic inputs from the adjacent continental areas during the transgression. The $\delta^{13}C$ values at the base of the sequence showed a decreasing trend with slight fluctuations between decreasing and increasing values (Fig. 6), as Salama et al. (2016) stated that is an indicator of the submarine lithification on the maximum flood surface. In addition, the changes in trophic conditions were probably as Salama et al. (2016) stated that reflected by the change in carbon isotopes.

Conclusions

The limestones of the Bozdağ Formation have developed as a reefal complex (stromatoporoid-coral patch reef) in a carbonate platform environment.

The major and trace element characteristics of the Bozdağ limestones show insignificant diagenetic alteration and an insignificant amount of terrigenous input. The source of the

terrigenous input observed in the Bozdağ limestone samples is predominantly felsic but originates from mixed provenance. The Zr ratio in most of the Bozdağ limestone samples shows that terrestrial pollution is low. Th/U ratios of the Bozdağ limestones show that there is no phosphate contamination in our samples and phosphates are taken from terrestrial input. The strong positive correlations between K_2O and TiO_2, K_2O and Al_2O_3, and TiO_2 and Al_2O_3 indicate that TiO_2 and K_2O are mainly from aluminosilicate clastics (clays). Correlations between Al_2O_3 of the Bozdağ limestone and immobile trace elements Zr and Th indicate that these elements are of terrestrial origin. Correlations of Al_2O_3 with Fe_2O_3 and MnO in the Bozdağ limestone samples show that Fe and Mn are partially derived from clays, although they mainly originate from sea waters. The rare earth element input is associated with detrital silicates and alumino-silicate inputs, not with the carbonate phase. In addition, during the precipitation of the Bozdağ limestones, the most terrigenous inputs were at the meters of 47 (J-28), 40 (J-24), and 62^{sd} (J-37), respectively.

C-values of the Bozdağ limestone samples show arid climate as paleoclimate. Furthermore, as the source of the terrestrial input in the Bozdağ limestone samples indicates the humid and arid climate region, the terrigenous material coming into the basin during the deposition of the Bozdağ limestones refers to climatic changes (humid to arid). In addition, during the precipitation of the Bozdağ limestones, terrestrial input was mostly eolian according to Al/Ti ratios.

During the deposition of the Bozdağ limestones, 8 samples suggest deposition under oxic environment conditions, while 19 samples suggest deposition under anoxic environment conditions. In the Ce/Ce* anomaly versus Al_2O_3, Fe_2O_3, and MnO diagram of the Bozdağ limestone samples, all samples emphasize the open sea environment in terms of sedimentation environment. In addition, the Ce values of the Bozdağ limestone samples are true negative values, indicating transgressive carbonate precipitation and anoxic precipitation rather than oxic. The early Silurian to Late Devonian period is also an inter-glacial stage in the region, supporting transgressive development.

The positive correlation between Ce anomaly with Fe_2O_3 and MnO of the Bozdağ limestone samples showed that there was no hydrothermal effect in the samples. Furthermore, the observation of Ce anomaly values in the Bozdağ limestone samples between 0.13 and 0.43 reflects the seawater feature. The Eu/Eu* values of the Bozdağ limestone samples are compatible with the open sea limestone values. In addition, the Y/Ho ratios of the Bozdağ Formation limestones have a relatively lower average value than the open seawater standard, which states that freshwater suspended load and/or wind-blown powders are effectively involved during the deposition of the Bozdağ limestones. These values also refer to some fluctuation in the water level. Again, the Y/Ho ratios of the Bozdağ limestones at values smaller than 102 (33 to 66) indicate that the conditions in the basin during their sedimentation were initially in the shallow shelf environment under oxic conditions, then in the deep shelf (open marine) anoxic conditions.

The Bozdağ limestone samples, according to the Mn/Sr ratio, have preserved their original seawater characteristics with isotope values. The Bozdağ limestone samples do not show any metamorphism effect according to K/Rb ratios. The Bozdağ limestones exhibit depletion by rare earth elements and not being affected by hydrothermal fluids. No correlation was observed between $\delta^{18}O$ and $\delta^{13}C$ isotope values and Mn/Sr ratios in the Bozdağ limestone samples, and the limestone samples retained their original values and did not undergo any significant alteration due to diagenesis. The $\delta^{18}O$ isotope values of Bozdağ limestone samples show that sudden increases and decreases in the middle and upper levels of the sequence in the mesodigenetic process, in some levels from the bottom to the top of the sequence, indicate that they are under geothermal effect; the fluctuations in the increase and decrease of $\delta^{18}O$ values in our samples indicate that they are caused by the effect of isotopic heavy and light fluids. While the change in the $\delta^{18}O$ values develops with the effect of buried temperature increase and geothermal liquids, we can say that the changes in the $\delta^{13}C$ values (increase-decrease) vary depending on climate changes (hot-cold), biological productivity, and partially terrestrial input.

Acknowledgment

The research was funded by the Selcuk University Scientific Research Fund (BAP) as part of Project 17201155. We thank the Research Fund of Selcuk University.

References

Abedini, A., Calagari, A.A., 2015. Rare earth element geochemistry of the Upper Permian limestone: the Kanigorgeh mining district, NW Iran. Turkish Journal of Earth Sciences 24, 365-382.

Abedini, A., Calagari, A.A., Rezaei, A.M., 2018. The tetrad-effect in rare earth elements distribution patterns of titanium-rich bauxites: evidence from the Kanigorgeh deposit, NW Iran. J. Geochem Explor. 186, 129-142.

Al-Aasm, I.S., Veizer, J., 1986. Diagenetic stabilization of aragonite and low-Mg calcite. II. Stable isotopes in rudists. Journal of Sedimentary Research 56, 763–770.

Ali, A., Wagreich, M., 2017. Geochemistry, environmental and provenance study of the Middle Miocene Leitha limestones (Central Paratethys). Geologica Carpathica 68(3), 248-268.

Armstrong-Altrin, J.S., Lee, Y.I., Verma, S.P., Worden, R.H., 2009. Carbon, oxygen, and strontium isotope geochemistry of carbonate rocks of the Upper Miocene Kudankulam Formation, Southern India: implications for paleoenvironment and diagenesis. Chem. Erde Geochem. 69(1), 45-60.

Bau, M., Dulski, P., 1996. Distribution of yttrium and rare-earth elements in the Penge and Kuruman iron-formations, Transvaal Supergroup. Precambrian Res. 79, 37-55.

Bau, M., Möller, P., Dulski, P., 1997. Yttrium and lanthanides in eastern Mediterranean seawater and their fractionation during redox-cycling. Mar. Chem. 56, 123-131.

Bauernhofer, A., Hauzenberger, C., Wallbrecher, E., Muhongo, S., Hoinkes, G., Mogessie, A., Opiyo-Akech, N., Tenczer, V., 2009. Geochemistry of basement rocks from SE Kenya and NE Tanzania: indications for rifting and early Pan-African subduction. International Journal of Earth Sciences 98(8), 1809-1834.

Bellanca, A., Masetti, D., Neri, R., 1997. Rare earth elements in limestone/marlstone couplets from the Albian-Cenomanian Cismon section (Venetian region, northern Italy): assessing REE sensitivity to environmental changes. Chemical Geology 141(3), 141-152.

Brand, U., Veizer, J., 1980. Chemical diagenesis of a multicomponent carbonate system: trace elements. Jour. Sediment. Petrol. 50, 1219-1236.

Brand, U., Veizer, J., 1981. Chemical diagenesis of a multicomponent carbonate system; 2, Stable isotopes. Journal of Sedimentary Research 51(3), 987-997.

Cao, J., Wu, M., Chen, Y., Hu, K., Bian, L.Z., Wang, L.G., Zhang, Y., 2012. Trace and rare earth element geochemistry of Jurassic mudstones in the northern Qaidam Basin, northwest China. Chem. Erde-Geochem. 72, 245-252.

Chen, L., Lin, A.T.S., Da, X., Yi, H., Tsai, L.L.Y., Xu, G., 2012. Sea-level changes recorded by cerium anomalies in the Late Jurassic (Tithonian) Black Rock Series of Qingtang Basin, North-Central Tibet. Oil Shale 29(1), 18-35.

Craigie, N.W., 2015. Applications of chemostratigraphy in Middle Jurassic unconventional reservoirs in eastern Saudi Arabia. GeoArabia 20(2), 79-110.

De Baar, H.J.W., German, C.R., Elderfield, H., 1988. Rare-earth element distributions in anoxic waters of the Cariaco Trench. Geochim. Cosmochim. Acta 52, 1203-1219.

Delpomdor, F., Préat, A., 2013. Early and late Neoproterozoic C, O and Sr isotope chemostratigraphy in the carbonates of West Congo and Mbuji-Mayi supergroups: A preserved marine signature? Palaeogeography, Palaeoclimatology, Palaeoecology 389, 35-47.

Ding, J., Zhang, J., Tang, X., Huo, Z., Han, S., Lang, Y., Zhang, Y., Li, X., Liu, T., 2018. Elemental geochemical evidence for depositional conditions and organic matter enrichment of Black Rock Series strata in an inter-platform basin: the Lower Carboniferous Datang Formation, Southern Guizhou, Southwest China. Minerals 8(11), 1-29.

Dunham, R.J., 1962. Classification of carbonate rocks according to depositional texture. AAPG Bull. 1, 108-121.

El-Bialy, M.Z., 2013. Geochemistry of the Neoproterozoic metasediments of Malhaq and Um Zariq Formations, Kid Metamorphic Complex, Sinai, Egypt: implications for source-area weathering, provenance, recycling, and depositional tectonic setting. Lithos 175-176, 68-85.

Elderfield, H., Greaves, M.J., 1982. The rare earth elements in seawater. Nature 296, 214-219.

Elderfield, H., 1988. The oceanic chemistry of the rare earth elements. Philos. Trans. R. Soc. Lond. A 325, 105-126.

Eren, Y., 1993. Eldeş-Derbent-Tepeköy-Söğütözü (Konya) Bölgesinin Jeolojisi, S.Ü. Doktora Tezi, Konya, p. 224 (Unpublished).

Eren, Y., 1996. Ilgın-Sarayönü (Konya) güneyinde Bozdağlar Masifinin stratigrafisi ve jeoloji evrimi. Jeoloji Mühendisliği Bölümü 30. Yıl Sempozyumu Bildirileri 1996, KTÜ Trabzon, (Eds: S. Korkmaz and M. Akçay), pp. 694-707.

Frimmel, H.E., 2009. Trace element distribution in Neoproterozoic carbonates as a paleoenvironmental indicator. Chemical Geology 258, 338-353.

Fritz, P., Smith, D.G.W., 1970. The isotopic composition of secondary dolomites. Geochim. Cosmochim. Acta 34, 1161-1173.

Google-Maps: https://www.google.com/maps/@38.0369777,32.4285516,11.25z/data=!5m1!1e4

Göncüoğlu, M.C., 2012. An Introduction to the Paleozoic Anatolia with a NW Gondwanan perspective. In: Göncüoğlu, M.C. and Bozdoğan, N. (Eds.), Guidebook Paleozoic of Eastern Taurides. Turkish Assoc. Petrol. Geol., Spec. Publ. Ankara 7, 1-15.

Greaves, M.J., Elderfield, H., Sholkovitz, E.R., 1999. Aeolian sources of rare earth elements to the Western Pacific Ocean. Marine Chemistry 68, 31-38.

Hajikazemi, E., Al-Aasami, I.S., Coniglio, M., 2010. Subaerial exposure and meteoric diagenesis of the Cenomanian–Turonian Upper Sarvak Formation, southwestern Iran, Geological Society, London, Special Publications 330, 253-272.

Haskin, L.A., Wildeman, T.R., Haskin, M.A., 1968. An accurate procedure for the determination of the rare earths by neutron activation. *Journal of Radioanalytical Chemistry* **1**, 337-348.

Hatch, J.R., Leventhal, J.S., 1992. Relationship between Inferred Redox Potential of the Depositional Environment and Geochemistry of the Upper Pennsylvanian (Missourian) Stark Shale Member of the Dennis Limestone, Wabaunsee Country, Kansas, USA. Chemical Geology 99, 65-82.

Hudson, J.D., 1977. Stable isotopes and limestone lithification. Jour. Geol. Soc. London 133, 637-660.

Joachimski, M.M., Breisig, S., Buggisch, W., Talent, J.A., 2009. Devonian climate and reef evolution: Insights from oxygen isotopes in apatite. Earth and Planetary Science Letters 284, 599-609.

Johannesson, K.H., Hawkins, Jr., D.L., Corte´s, A., 2006. Do Archean chemical sediments record ancient seawater rare earth element patterns? Geochim. Cosmochim. Acta 70, 871-890.

Jones, B., Manning, D.A.C., 1994. Comparison of geochemical indices used for the interpretation of palaeoredox conditions in ancient mudstones. Chemical Geology 111(1-4), 111-129.

Kuchenbecker, M., Babinski, M., Pedrosa-Soares, A.C., Lopes-Silva, L., Pimenta, F., 2016. Chemostratigraphy of the Lower Bambuí Group, Southwestern São Francisco Craton, Brazil: insights on Gondwana paleoenvironments. Brazilian Journal of Geology 46, 145-162.

Lawrence, M.G., Greig, A., Collerson, K.D., Kamber, B.S., 2006. Rare-earth element and yttrium variability in South East Queens-land waterways. Aquatic Geochemistry 12(1), 39-72.

Madhavaraju, J., Pacheco-Olivas, S.A., Gonzalez-Leon, C.M., Espinoza-Maldonado, I.G., Sanchez-Medrano, P.A., Villanueva-Amadoz, U., Monreal, R., Pi-Puig, T., Ramirez-Montoya, E., Grijalva-Noriega, F.J., 2017. Clay mineralogy and geochemistry of the Lower Cretaceous siliciclastic rocks of the Morita Formation, Sierra San José section, Sonora, Mexico. J S Am. Earth. Sci. 76, 397-411.

Maity, B., Indares, A., 2018. The Geon 14 arc-related mafic rocks from the Central Grenville Province. Canadian Journal of Earth Sciences 55(6), 545-570.

McLennan, S.M., 1989. Rare earth elements in sedimentary rocks: influence of provenance and sedimentary process. Review of Mineralogy 21, 169-200.

Murphy, K., Dymond, J., 1984. Rare earth element fluxes and geochemical budget in the eastern Equatorial Pacific. Nature 307, 444-447.

Murray, R.W., Brink, M.R.B., Brumsack, H.J., Gerlach, D.C., 1991. Rare earth elements in Japan Sea sediments and diagenetic behavior of Ce/Ce∗: results from ODP Leg 127. Geochim. Cosmochim. Acta 55(9), 2453-2466.

Nakamura, K., 2015. Chemostratigraphy of the Late Cretaceous Western Interior (Greenhorn, Carlile, and Niobrara Formations), Denver Basin, co U.S.A., the Faculty and the Board of Trustees of the Colorado School of Mines in partial fulfillment of the requirements for the degree of Doctorate of Philosophy (Geology). Golden, Colorado, p. 93.

Nothdurft, L., Webb, G.E., Kamber, B.S., 2004. Rare earth element geochemistry of Late Devonian reefal carbonates, Canning Basin, Western Australia: confirmation of a seawater REE proxy in ancient limestones. Geochimica et Cosmochimica Acta 68, 263-283.

Özkan, A.M., 2016. Söğütözü-Ladik (Konya) çevresindeki Bozdağ Formasyonu (Silüriyen-Alt Karbonifer) dolomitlerinin sedimantolojik ve jeokimyasal incelenmesi. Selçuk Üniversitesi BAP Proje No: 11201124, p. 124 (Unpublished).

Piepgras, D.J., Jacobsen, S.B., 1992. The behavior of rare earth elements in seawater: precise determination of variations in the North Pacific water column. Geochim. Cosmochim. Acta 56, 1851-1862.

Ratcliffe, K., Montgomery, P., Palfrey, A., Vonk, A., 2010. Application of chemostratigraphy to the Mungaroo Formation, the Gorgon Field, offshore Northwest Australia. The APPEA Journal 50(1), 371-386.

Roy, D.K., Roser, B.P., 2013. Climatic control on the composition of Carboniferous-Permian Gondwana sediments, Khalaspir Basin, Bangladesh. Gondwana Res. 23, 1163-1171.

Rudnick, R.L., McLennan, S.M., Taylor, S.R., 1985. Large iron lithophile elements in rocks from high-pressure granulite facies terrains. Geochim. Cosmochim. Acta 49,1645-1655.

Salama, Y.F., Abdel-Gawad, G.I., Saber, S.G., El-Shazly, S.H., Grammer, G.M., Özer, S., 2016. Chemostratigraphy of the Cenomanian-Turonian shallow-water carbonate: new correlation for the rudist levels from North Sinai, Egypt. Arab Jour. Geosci 9(755), 1-18.

Sholkovitz, E.R., 1988. Rare earth elements in the sediments of the North Atlantic Ocean, Amazon Delta, and East China Sea: reinterpretation of terrigenous input patterns to the oceans. American Journal of Science 288(3), 236-281.

Song, C., Herong, G., Linhua, S., 2014. Geochemical characteristics of REE in the Late Neo-Proterozoic limestone from northern Anhui Province, China. Chin Jour. Geochem. 33, 187-193.

Taylor, S.R., McLennan, S.M., 1985. The continental crust: its composition and evolution. Blackwell, Cambridge pp. 312.

Thurston, G.D., Ito, K., Lall, R., 2011. A source apportionment of US fine particulate matter air pollution. Atmospheric Environment 45(39), 24-36.

Tsegab, H., Sum, C.W., 2019. Chemostratigraphy of Paleozoic Carbonates in the Western Belt (Peninsular Malaysia): A Case Study on the Kinta Limestone. IntechOpen, 1-24.

Van Geldern, R., Joachimski, M.M., Day, J., Jansen, U., 2006. Carbon, oxygen and strontium isotope records of Devonian brachiopod shell calcite. Palaeogeography Palaeoclimatology Palaeoecology 240(1), 47-67.

Wang, Z.W., Fu, X.G., Feng, X.L., Song, C., Wang, D., Chen, W.B., Zeng, S.Q., 2017. Geochemical features of the black shales from the Wuyu Basin, southern Tibet: implications for palaeoenvironment and palaeoclimate. Geol. Jour. 52, 282-297.

Wilde, P., Quinby-Hunt, M.S., Erdtmann, B.D., 1996. The Whole-rock cerium anomaly: a potential indicator of eustatic sea-level changes in shales of the anoxic facies. Sediment. Geol. 101(1-2), 43-53.

Wronkiewic, D.J., Condie, K.C., 1987. Geochemistry of Archean shales from the Witwatersrand Supergroup, South Africa: source-area weathering and provenance. Geochimica et Cosmochimica Acta, 51(9), 2401-2416.

Xie, G.L., Shen, Y.L., Liu, S.G., Hao, W.D., 2018. Trace and rare earth element (REE) characteristics of mudstones from Eocene Pinghu Formation and Oligocene Huagang Formation in Xihu Sag, East China Sea Basin: implications for provenance, depositional conditions and paleoclimate. Mar. Petrol. Geol. 92, 20-36.

Zhang, K.J., Li, Q.H., Yan, L.L., Zeng, L., Lu, L., Zhang, Y.X., Hui, J., Jin, X., Tang, X.C., 2017. Geochemistry of limestones deposited in various plate tectonic settings. Earth-Science Reviews 167, 26-47.

Zhao, Y., Zheng, Y.F., Chen, F., 2009. Trace element and strontium isotope constraints on sedimentary environment of Ediacaran carbonates in southern Anhui, South China. Chemical Geology 265, 345-362.